Title
Reflective Cracking Study: Summary Report

Authors
Jones, David
Harvey, John T
Monismith, Carl L.

Publication Date
2008-10-01

Peer reviewed

December 2007
Summary Report: UCPRC-SR-2007-01

Reflective Cracking Study: Summary Report

Authors:
D. Jones, J. Harvey, and C. Monismith

Partnered Pavement Research Program (PPRC) Contract Strategic Plan Element 4.10:
Development of Improved Rehabilitation Designs for Reflective Cracking

PREPARED FOR:

California Department of Transportation
Division of Research and Innovation
Office of Roadway Research

PREPARED BY:

University of California
Pavement Research Center
UC Davis, UC Berkeley

DOCUMENT RETRIEVAL PAGE		**Summary Report: UCPRC-SR-2007-01**
Title: Reflective Cracking Study: Summary Report		
Authors: D. Jones, J. Harvey and C. Monismith		
Prepared for: Caltrans	**FHWA No:** CA091073N	**Date:** December 2007
Contract No: 65A0172	**Client Reference No:** SPE 4.10	**Status:** Stage 6, Approved Version

Abstract:
This report summarizes a series of eight first-level Heavy Vehicle Simulator testing reports, two laboratory reports on shear and fatigue testing, a forensic investigation report, a report on the backcalculation of deflection measurements, and a second-level analysis report, all of which document an investigation undertaken to validate Caltrans overlay strategies for the rehabilitation of cracked asphalt concrete using modified binder overlays.

The work was conducted by the University of California Pavement Research Center (UCPRC) as part of Partnered Pavement Research Center Strategic Plan Element 4.10: "Development of Improved Rehabilitation Designs for Reflective Cracking." This work was originally requested by the Caltrans/Industry Rubber Asphalt Concrete Task Group (RACTG) to compare the performance of one set of examples of thin overlays of cracked asphalt pavement containing different types of binders modified with recycled tire rubber. This work, included as Appendix H of the Rubber Modified Binder Pilot Projects Review prepared by the RACTG, is part of a more comprehensive work plan prepared by the Task Group that included evaluation of pilot projects and construction and monitoring of field test sections (undertaken by Caltrans).

The objective of this UCPRC project was met after completion of the following four tasks:

1. Develop improved mechanistic models of reflective cracking in California,
2. Calibrate and verify these models using laboratory and HVS testing,
3. Evaluate the most effective strategies for reflective cracking, and
4. Provide recommendations for reflective cracking strategies.

This report addresses all the tasks and consists of six main chapters. Chapter 2 lists the objectives and project organization. Chapter 3 provides an overview of the experiment details. Chapters 4 and 5 summarize HVS and laboratory testing, respectively. Chapter 6 discusses the second-level analysis. Chapter 7 lists key findings of the study and provides recommendations for implementation.

Keywords:
Reflective cracking, overlay, modified binder, HVS test, MB Road, forensic investigation

Related documents:
UCPRC-WP-2003-01, UCPRC-RR-2005-03, RR-2006-04, RR-2006-05, RR-2006-06, RR-2006-07, RR-2006-08, RR-2006-11, RR-2006-12, RR-2007-04, RR-2007-05, RR-2007-08, RR-2007-09

Signatures:

D. Jones **1st Author**	J. Harvey **Technical Review**	D. Spinner **Editor**	J. Harvey **Principal Investigator**	M. Samadian **Caltrans Contract Manager**

DISCLAIMER

The contents of this report reflect the views of the authors who are responsible for the facts and accuracy of the data presented herein. The contents do not necessarily reflect the official views or policies of the State of California or the Federal Highway Administration. This report does not constitute a standard, specification, or regulation.

PROJECT OBJECTIVES

The objective of this project is to develop improved rehabilitation designs for reflective cracking for California.

This objective will have been met after completion of four tasks identified by the Caltrans/Industry Rubber Asphalt Concrete Task Group (RACTG):

1. Develop improved mechanistic models of reflective cracking in California,
2. Calibrate and verify these models using laboratory and HVS testing,
3. Evaluate the most effective strategies for reflective cracking, and
4. Provide recommendations for reflective cracking strategies.

This document addresses all these tasks.

ACKNOWLEDGEMENTS

The University of California Pavement Research Center acknowledges the assistance of the Rubber Pavements Association, Valero Energy Corporation, and Paramount Petroleum, which contributed funds and asphalt binders for the construction of the Heavy Vehicle Simulator test track discussed in this study.

REFLECTIVE CRACKING STUDY REPORTS

The reports prepared during the reflective cracking study document data from construction, Heavy Vehicle Simulator (HVS) tests, laboratory tests, and subsequent analyses. These include a series of first- and second-level analysis reports and two summary reports as follows:

1. Reflective Cracking Study: Summary of Construction Activities, Phase 1 HVS testing and Overlay Construction (UCPRC-RR-2005-03).
2. Reflective Cracking Study: First-level Report on the HVS Rutting Experiment (UCPRC-RR-2007-06).
3. Reflective Cracking Study: First-level Report on HVS Testing on Section 590RF — 90 mm MB4-G Overlay (UCPRC-RR-2006-04).
4. Reflective Cracking Study: First-level Report on HVS Testing on Section 589RF — 45 mm MB4-G Overlay (UCPRC-RR-2006-05).
5. Reflective Cracking Study: First-level Report on HVS Testing on Section 587RF — 45 mm RAC-G Overlay (UCPRC-RR-2006-06).
6. Reflective Cracking Study: First-level Report on HVS Testing on Section 588RF — 90 mm AR4000-D Overlay (UCPRC-RR-2006-07).
7. Reflective Cracking Study: First-level Report on HVS Testing on Section 586RF — 45 mm MB15-G Overlay (UCPRC-RR-2006-12).
8. Reflective Cracking Study: First-level Report on HVS Testing on Section 591RF — 45 mm MAC15-G Overlay (UCPRC-RR-2007-04).
9. Reflective Cracking Study: HVS Test Section Forensic Report (UCPRC-RR-2007-05).
10. Reflective Cracking Study: First-level Report on Laboratory Fatigue Testing (UCPRC-RR-2006-08).
11. Reflective Cracking Study: First-level Report on Laboratory Shear Testing (UCPRC-RR-2006-11).
12. Reflective Cracking Study: Backcalculation of FWD Data from HVS Test Sections (UCPRC-RR-2007-08).
13. Reflective Cracking Study: Second-level Analysis Report (UCPRC-RR-2007-09).
14. Reflective Cracking Study: Summary Report (UCPRC-SR-2007-01). Detailed summary report.
15. Reflective Cracking Study: Summary Report (UCPRC-SR-2007-03). Four-page summary report.

CONVERSION FACTORS

SI* (MODERN METRIC) CONVERSION FACTORS				
APPROXIMATE CONVERSIONS TO SI UNITS				
Symbol	**Convert From**	**Multiply By**	**Convert To**	**Symbol**
LENGTH				
in	inches	25.4	millimeters	mm
ft	feet	0.305	meters	m
AREA				
in^2	square inches	645.2	square millimeters	mm^2
ft^2	square feet	0.093	square meters	m2
VOLUME				
ft^3	cubic feet	0.028	cubic meters	m^3
MASS				
lb	pounds	0.454	kilograms	kg
TEMPERATURE (exact degrees)				
°F	Fahrenheit	5 (F-32)/9 or (F-32)/1.8	Celsius	C
FORCE and PRESSURE or STRESS				
lbf	poundforce	4.45	newtons	N
lbf/in^2	poundforce/square inch	6.89	kilopascals	kPa
APPROXIMATE CONVERSIONS FROM SI UNITS				
Symbol	**Convert From**	**Multiply By**	**Convert To**	**Symbol**
LENGTH				
mm	millimeters	0.039	inches	in
m	meters	3.28	feet	ft
AREA				
mm^2	square millimeters	0.0016	square inches	in^2
m^2	square meters	10.764	square feet	ft^2
VOLUME				
m^3	cubic meters	35.314	cubic feet	ft^3
MASS				
kg	kilograms	2.202	pounds	lb
TEMPERATURE (exact degrees)				
C	Celsius	1.8C+32	Fahrenheit	F
FORCE and PRESSURE or STRESS				
N	newtons	0.225	poundforce	lbf
kPa	kilopascals	0.145	poundforce/square inch	lbf/in^2

*SI is the symbol for the International System of Units. Appropriate rounding should be made to comply with Section 4 of ASTM E380.
(Revised March 2003)

TABLE OF CONTENTS

LIST OF TABLES

LIST OF FIGURES

1. INTRODUCTION

The California Department of Transportation (Caltrans) operates a state highway network of more than 78,000 lane-kilometers (49,000 lane miles), 68 percent of which is flexible pavement (asphalt concrete). Like most other states in the U.S.A., this network can be considered as mature, requiring ongoing maintenance and rehabilitation. Traffic on the flexible pavement network ranges from relatively light traffic on some of the state routes to very heavy traffic on the interstate highways and urban truck routes. The condition of the roads varies. Fatigue, reflected fatigue, and thermal cracking are common distresses, with the degree of severity depending on the age of the road, the underlying structure, traffic volume, and climate. Maintenance treatments typically involve thin overlays, while rehabilitation and structural improvements typically involve thicker overlays. These overlays are either dense- or open-graded asphalt concrete (hot-mix asphalt), or gap- or open-graded rubberized asphalt concrete. Previous research has shown that use of asphalt rubber binders in gap-graded mixes allows for a reduction in the thickness of overlays of up to 50 percent compared with conventional binders in dense-graded mixes, without detriment to fatigue performance or crack reflection.

California started using rubberized asphalt concrete (RAC) in the 1970s, based on the experience of transportation departments in Arizona and in other countries, and the practice is now common in the state. Historically, a recipe specification for field blending the binder and rubber was used in order to counter the asphalt rubber binders' relatively short shelf lives. However recent developments in blending at the refinery and the adoption of performance-based specifications for hot-mix asphalt (HMA) by the Strategic Highway Research Program (SHRP) prompted a study to develop and implement performance-based specifications for these mixes in California. A Caltrans/Industry Rubber Asphalt Concrete Task Group (RACTG) was established to oversee the study, which included evaluation of pilot projects, laboratory testing, Heavy Vehicle Simulator (HVS) testing, and construction and monitoring of field test sections.

This report is a summary of the HVS and laboratory testing components and the analysis of the results, conducted by the University of California Pavement Research Center as part of Partnered Pavement Research Center Strategic Plan Element 4.10: "Development of Improved Rehabilitation Designs for Reflective Cracking."

2. OBJECTIVES AND PROJECT ORGANIZATION

2.1. Objectives

The study described in this report is part of Partnered Pavement Research Center Strategic Plan Element 4.10 (PPRC SPE 4.10) being undertaken for the California Department of Transportation (Caltrans) by the University of California Pavement Research Center (UCPRC). This work is part of a larger study on modified binder (MB) mixes being carried out under the guidance of the Caltrans Pavement Standards Team (PST) (1) that includes laboratory and accelerated pavement testing using the Heavy Vehicle Simulator (carried out by the UCPRC), and the construction and monitoring of field test sections (carried out by Caltrans).

The objective of the study (SPE 4.10) was to evaluate the reflective cracking performance of three modified asphalt binder mixes used in overlays for rehabilitating cracked asphalt concrete pavements in California, and will have been met after completion of the following four tasks identified by the Caltrans/Industry Rubber Asphalt Concrete Task Group (RACTG):

1. Develop improved mechanistic models of reflective cracking in California,
2. Calibrate and verify these models using laboratory and HVS testing,
3. Evaluate the most effective strategies for reflective cracking, and
4. Provide recommendations for reflective cracking rehabilitation strategies.

The following three gap-graded modified binder mixes were selected by the RACTG based on the evaluation of pilot projects:

- MB4-G;
- MB4-G with minimum 15 percent recycled tire rubber, and
- MAC15TR-G with minimum 15 percent recycled tire rubber.

Performance was compared against that of a dense-graded mix with a conventional binder (approximately equivalent to PG64-16) and a gap-graded rubberized asphalt concrete mix, included for control purposes.

2.2. Overall Project Organization

This UCPRC project was a comprehensive study, carried out in three phases between 2001 and 2007, involving the following primary elements (2):

- Phase 1
  - The construction of a test pavement and subsequent overlays;
  - Six separate Heavy Vehicle Simulator (HVS) tests to crack the pavement structure;
  - Placing of six different overlays on the cracked pavement;
- Phase 2
  - Six HVS tests that assessed the susceptibility of the overlays to high-temperature rutting (Phase 2a);
  - Six HVS tests to determine the low-temperature reflective cracking performance of the overlays (Phase 2b);
  - Laboratory shear and fatigue testing of the various hot-mix asphalts (Phase 2c);
  - Falling Weight Deflectometer (FWD) testing of the test pavement before and after construction and before and after each HVS test;
  - Forensic evaluation of each HVS test section;
- Phase 3
  - Performance modeling and simulation of the various mixes using models calibrated with data from the primary elements listed above.

An overview of the project timeline is shown in Figure 2.1.

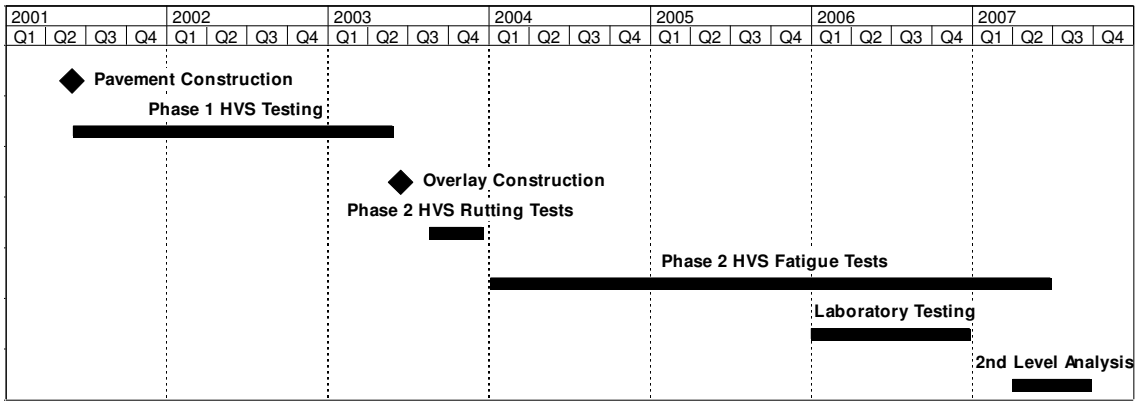

Figure 2.1: Timeline for the Reflective Cracking Study.

2.3. Reports

The reports prepared during the reflective cracking study document data from construction, HVS tests, laboratory tests, and subsequent analyses. These include a series of first- and second-level analysis reports and two summary reports. On completion of the study this suite of documents will include:

- One first-level report covering the initial pavement construction, the six initial HVS tests, and the overlay construction (Phase 1);
- One first-level report covering the six Phase 2 rutting tests (but offering no detailed explanations or conclusions on the performance of the pavements);
- Six first-level reports, each of which covers a single Phase 2 reflective cracking test (containing summaries and trends of the measured environmental conditions, pavement responses, and pavement performance but offering no detailed explanations or conclusions on the performance of the pavement);
- One first-level report covering laboratory shear testing;
- One first-level report covering laboratory fatigue testing;
- One report summarizing the HVS test section forensic investigation;
- One report summarizing the backcalculation analysis of deflection tests,
- One second-level analysis report detailing the characterization of shear and fatigue data, pavement modeling analysis, comparisons of the various overlays, and simulations using various scenarios (Phase 3), and
- One four-page summary report capturing the entire study's conclusions and one longer, more detailed summary report that covers the findings and conclusions from the research conducted by the UCPRC.

2.4. Structure and Content of this Report

This report presents a summary of the entire study, and is based on the contents of the reports listed above. The report is organized as follows:

- Chapter 3 contains an overview of the HVS and laboratory test programs,
- Chapter 4 summarizes the findings from the Phase 1 and Phase 2 HVS tests,
- Chapter 5 summarizes the findings from the laboratory fatigue and shear tests,
- Chapter 6 summarizes the findings from the second-level analysis, and
- Chapter 7 provides conclusions and recommendations from the study.

3. EXPERIMENT DETAILS

3.1. Test Track Location, Design and Construction

The test track for this study was located at the University of California, Berkeley, Richmond Field Station (Figures 3.1 and 3.2).

The pavement was designed according to the Caltrans Highway Design Manual Chapter 600 using the computer program *NEWCON90.* Design thickness was based on a tested subgrade R-value of 5 and a Traffic Index of 7 (~121,000 ESALs) (3).

During construction, the existing subgrade was ripped and reworked to a depth of 200 mm (4 in.) so that the optimum moisture content and the maximum wet density met the specification per Caltrans Test Method, CTM 216. The average maximum wet density of the subgrade was 2,180 kg/m^3 (136 pcf). The average relative compaction of the subgrade was 97 percent (3).

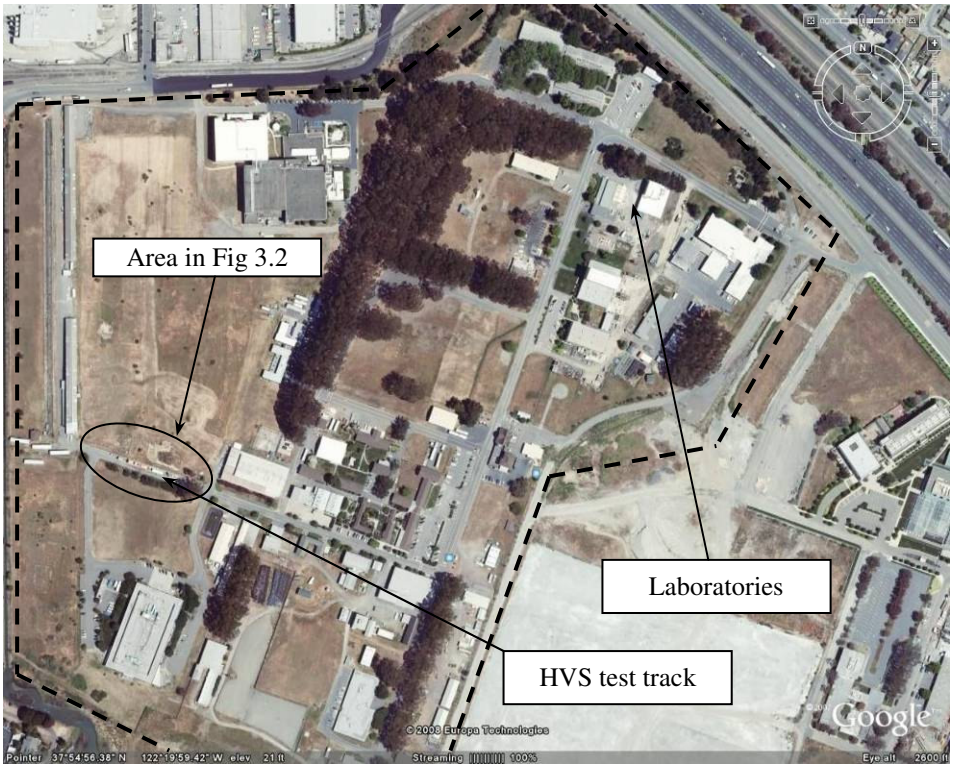

Figure 3.1: Location of HVS test track at Richmond Field Station. (1)

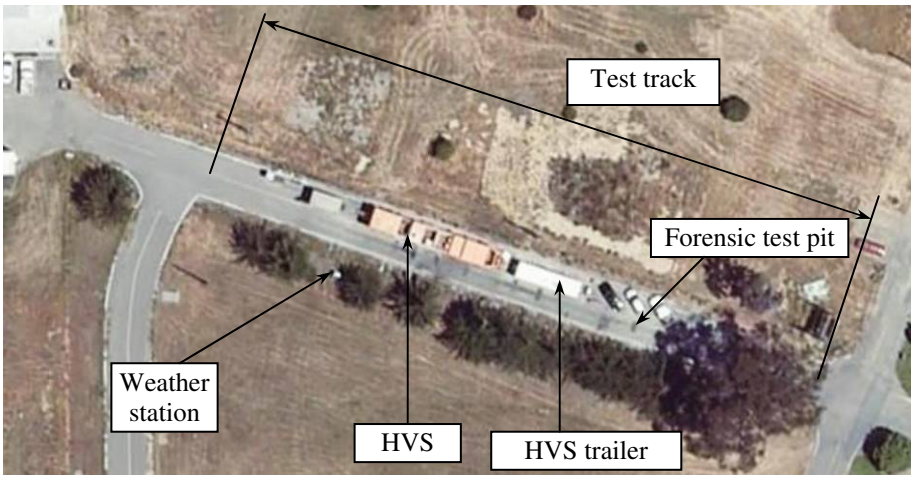

Figure 3.2: Location of HVS test track at Richmond Field Station. (2)

The aggregate base was constructed to meet the Caltrans compaction requirements for Class 2 aggregate base using CTM 231 nuclear density testing. The average maximum wet density of the base determined according to CTM 216 was 2,200 kg/m^3 (137 pcf). The average relative compaction was 98 percent.

The wearing course layer for Phase 1 HVS testing consisted of dense-graded asphalt concrete (DGAC) with AR-4000 binder (approximately equivalent to a PG64-16 performance grade binder) and aggregate gradation limits following Caltrans 19-mm (0.75-in.) maximum size coarse gradation (3). The target asphalt content was 5.0 percent by mass of aggregate, while actual contents varied between 4.34 and 5.69 percent. Nuclear density measurements and extracted cores were used to determine a preliminary as-built mean air-void content of 9.1 percent with a standard deviation of 1.8 percent. The base was primed before placing the asphalt concrete.

Six HVS test sections (567RF to 569RF and 571RF to 573RF) were demarcated on the surface for Phase 1 HVS testing (Figure 3.3 [Test track - before overlay]). HVS testing is discussed in Chapter 4.

The overlay thickness for Phase 2 HVS testing was determined according to Caltrans Test Method CTM 356 using Falling Weight Deflectometer data collected after completion of the Phase 1 testing. The design thickness for the conventional DGAC overlay, included for control purposes, was 90 mm (3.5 in.). The various modified overlays were either full (90 mm [3.5 in.]) or half thickness (45 mm [1.7 in.]). Mixes were designed by Caltrans. The six overlays were placed in one day, within a few hours of each other. A tack coat was applied prior to placement. The 90-mm layers were placed in two lifts of 45 mm and a tack coat was applied between lifts.

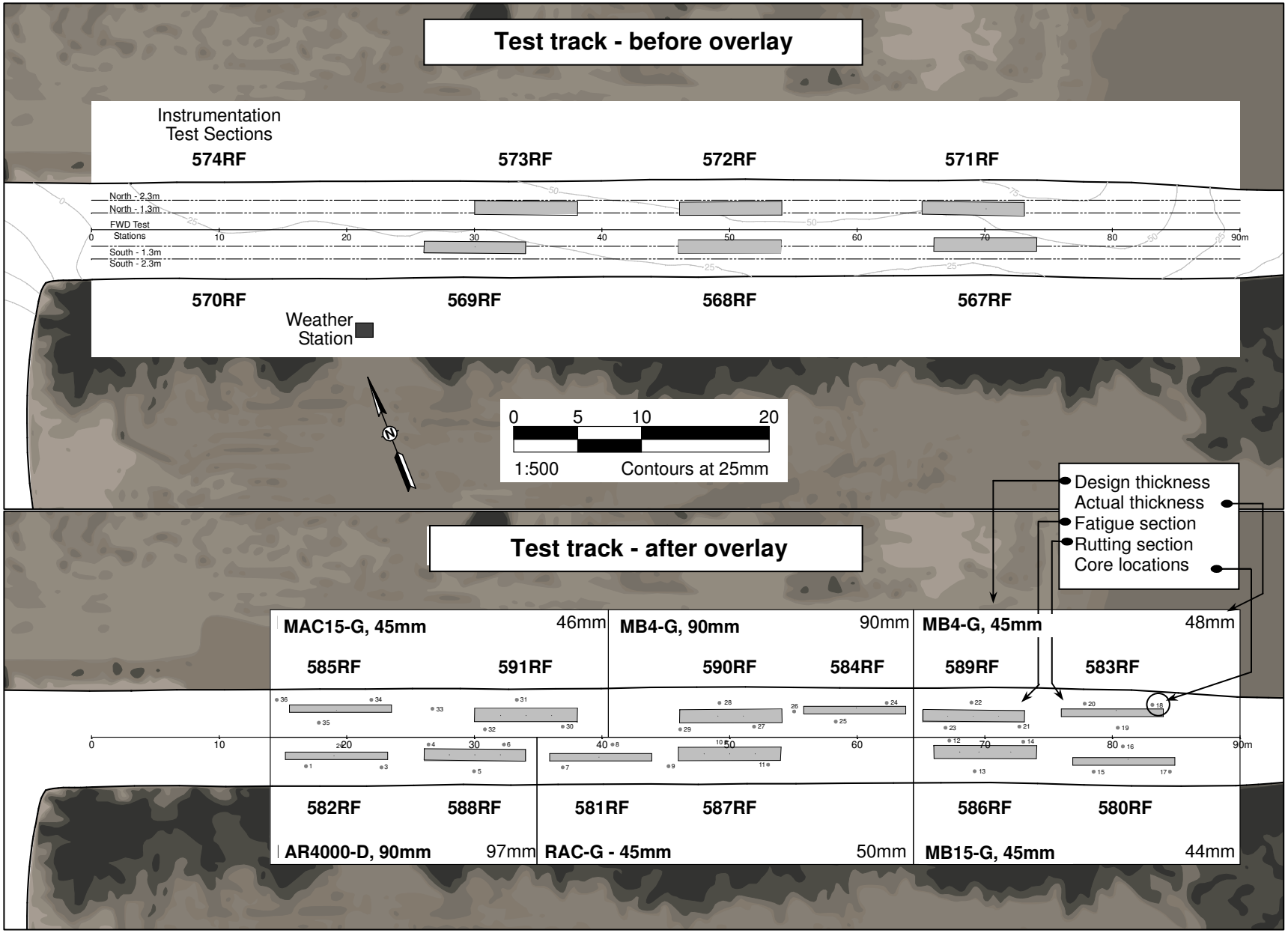

Figure 3.3: Layout of the Reflective Cracking Study test track.

Two test sections (one rutting and one reflective cracking) were demarcated on each overlay for Phase 2 HVS testing (Figure 3.3 [Test track - after overlay]). The section designations (rutting/reflective cracking) and descriptions were as follows:

1. 580RF/586RF: Half-thickness (45 mm) MB4 gap-graded overlay with minimum 15 percent recycled tire rubber ("MB15-G" in this report);
2. 581RF/587RF: Half-thickness (45 mm) rubberized asphalt concrete gap-graded overlay ("RAC-G");
3. 582RF/588RF: Full-thickness (90 mm) AR4000 dense-graded asphalt concrete overlay (designed using CTM 356 and referred to as "AR4000-D" in this report);
4. 583RF/589RF: Half-thickness (45 mm) MB4 gap-graded overlay ("45 mm MB4-G");
5. 584RF/590RF: Full-thickness (90 mm) MB4 gap-graded overlay ("90 mm MB4-G"), and
6. 585RF/591RF: Half-thickness (45 mm) MAC15TR gap-graded overlay with minimum 15 percent recycled tire rubber ("MAC15-G").

The pavement design and the as-built pavement structure for each Phase 2 test section are illustrated in Figure 3.4. As-built thicknesses were determined from cores removed from the edge of the sections, and then verified during test pit assessments on each section after HVS trafficking. Laboratory testing was carried out by Caltrans and UCPRC on samples collected during construction to determine actual binder properties, binder content, aggregate gradation, and air-void content.

The binders met requirements, based on testing performed by Caltrans. The average ignition-extracted binder contents of the various layers, corrected for aggregate ignition and compared to the design binder content, are listed in Table 3.1. For each section, actual binder contents were higher than design contents. It is not clear whether this is a function of the test or contractor error.

Table 3.1: Design versus Actual Binder Contents

Mix	Binder Content (%)	
	Design	Actual
MB15-G	7.1	7.52
RAC-G	8.0	8.49
AR4000-D	5.0	6.13
MB4-G (45 mm)	7.2	7.77
MB4-G (90 mm)	7.2	7.77
MAC15-G	7.4	7.55

The aggregate gradations for the dense- and gap-graded mixes generally met Caltrans specifications for 19.0 mm (0.75 in.) maximum size coarse and gap gradations respectively. Gradations are illustrated in Figure 3.5 (AR4000-D) and Figure 3.6 (modified binders).

Design	580RF/586RF	581RF/587RF	582RF/588RF	583RF/589RF	584RF/590RF	585RF/591RF
Overlay (45 or 90 mm)	MB15-G (46 mm)	RAC-G (50 mm)	AR4000-D (94 mm)	MB4-G (48 mm)	MB4-G (91 mm)	MAC15-G (45 mm)
DGAC (90 mm)	DGAC (81 mm)	DGAC (81 mm)	DGAC (93 mm)	DGAC (77 mm)	DGAC (88 mm)	DGAC (110 mm)
Class 2 Aggregate Base (410 mm)	Class 2 Aggregate Base (398 mm)	Class 2 Aggregate Base (398 mm)	Class 2 Aggregate Base (369 mm)	Class 2 Aggregate Base (372 mm)	Class 2 Aggregate Base (352 mm)	Class 2 Aggregate Base (411 mm)
Clay subgrade (semi-infinite)	Clay subgrade (semi-infinite)	Clay subgrade (semi-infinite)	Clay subgrade (semi-infinite)	Clay subgrade (semi-infinite)	Clay subgrade (semi-infinite)	Clay subgrade (semi-infinite)

Figure 3.4: Pavement design for Reflective Cracking Study experiment (design and actual).

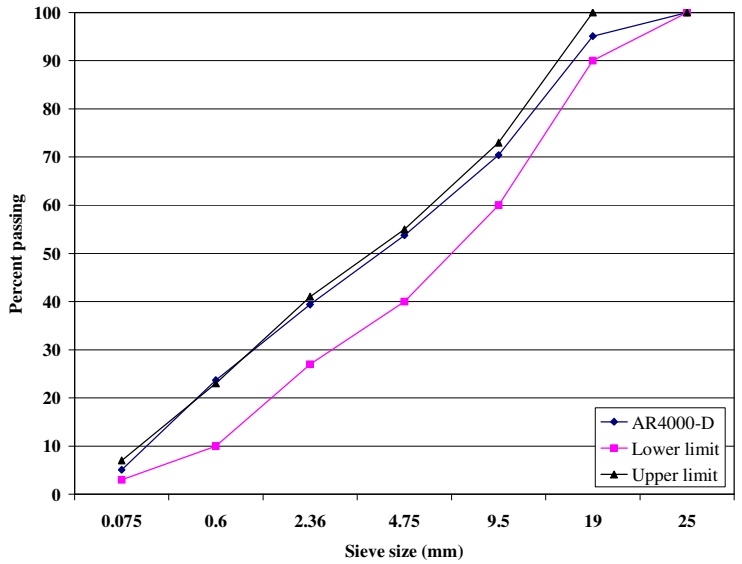

Figure 3.5: Gradation for AR4000-D overlay.

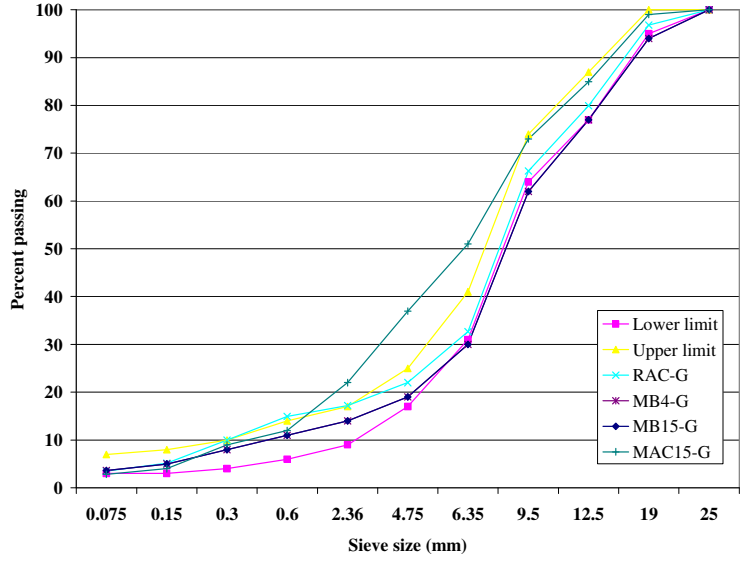

Figure 3.6: Gradation for modified binder overlays.

The preliminary as-built air-void contents for each section, based on cores taken outside of the HVS sections prior to HVS testing, together with the air-void contents determined from cores extracted from the HVS wheelpath on each reflective cracking testing section after HVS trafficking are listed in Table 3.2.

Table 3.2: Air-Void Contents

Overlay	Air-Void Content (%)			
	Average for Section		Standard Deviation	
	Before HVS Test	After HVS Test	Before HVS Test	After HVS Test
MB15-G	5.1	3.8	1.7	1.5
RAC-G	8.8	4.0	1.3	1.6
AR4000-D	7.1	6.5	1.5	1.6
MB4-G (45 mm)	6.5	2.9	0.6	1.2
MB4-G (90 mm)	6.5	1.9	0.6	0.7
MAC15-G	4.9	2.7	1.0	1.5

3.2. Test Section Layout and Pavement Instrumentation

The typical layout of a test section is shown in Figure 3.7. Station numbers refer to fixed points on the test section and are used for measurements and as a reference for discussing performance.

Measurements were taken with the following instruments:

- Road Surface Deflectometer (RSD), measuring surface deflection;
- Multi-depth Deflectometer (MDD), measuring elastic deflection and permanent deformation at different depths in the pavement;
- Laser Profilometer, measuring surface profile (at each station);
- Falling Weight Deflectometer (FWD), measuring elastic deflection before and after testing, and
- Thermocouples, measuring pavement temperature and ambient temperature.

Instrument positions are shown in Figure 3.7. Detailed descriptions of the instrumentation and measuring equipment are included in Reference 4.

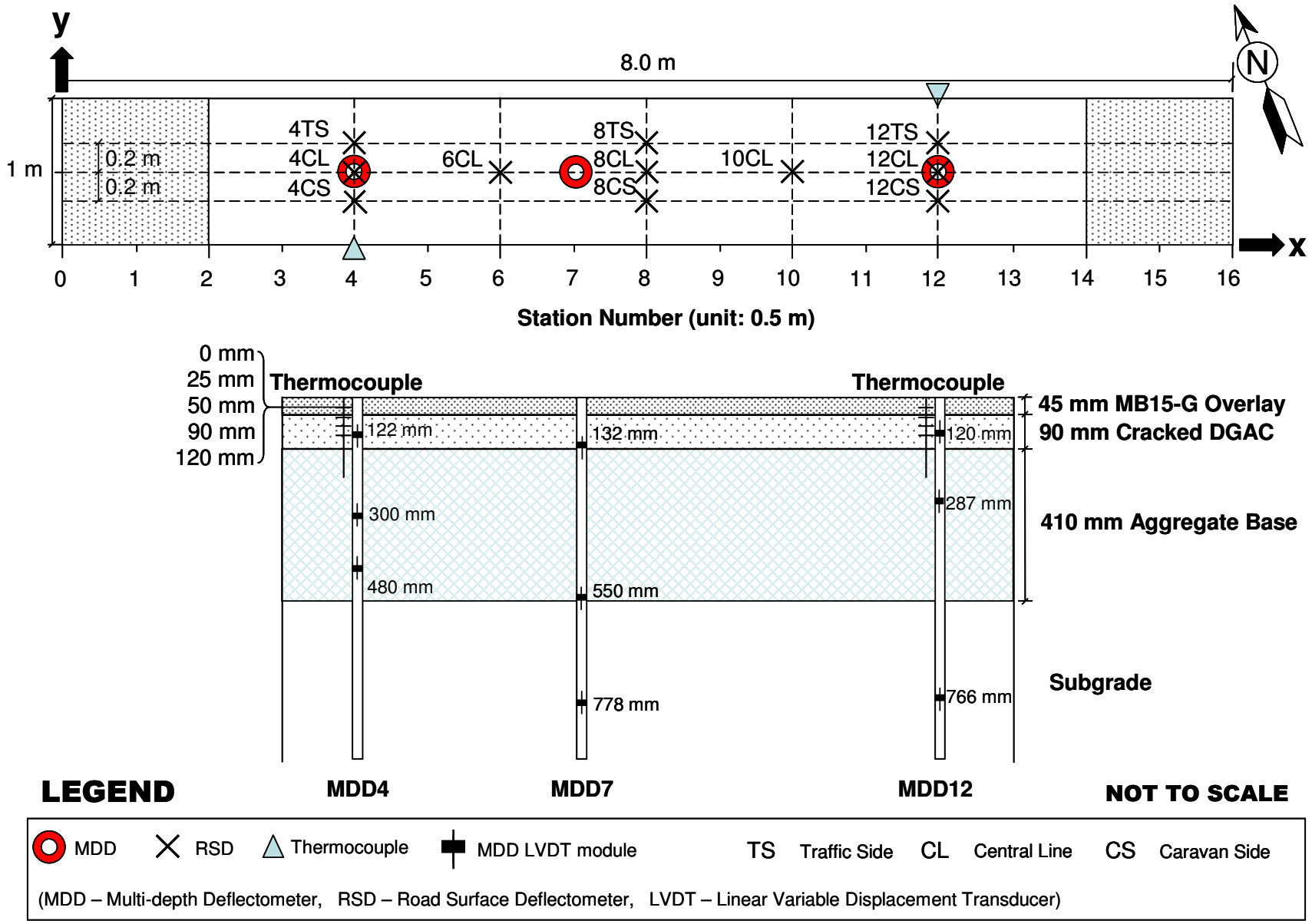

Figure 3.7: Typical layout of HVS test section.

4. HVS TESTING

4.1. Phase 1 HVS Testing

HVS testing on the underlying layer (Phase 1) is discussed in detail in one first-level analysis report (3).

The first phase of HVS trafficking was carried out on six test sections on the original DGAC layer to induce fatigue cracking. The sections were maintained at 20°C±4°C (68°F±7°F) using a temperature chamber. The failure criteria for the experiment were set at 2.5 m/m^2 (0.76 ft/ft^2) of fatigue cracking and/or 12.5 mm (0.5 in.) average maximum rut. HVS trafficking took place between December 21, 2001, and April 11, 2003, and is summarized in Table 4.1. The wide range of repetitions required to achieve the required crack density was attributed to variation in the base layer, which is discussed in Section 4.3. The implications of this variation on section performance are discussed in Chapter 6.

Table 4.1: Summary of Testing on the Underlying DGAC Layer

Section	Planned Overlay	Start Date	End Date	Load Repetitions	Wheel Load (kN)	Wheel	Tire Pressure (kPa)	Direction
567RF	MB15-G	12/21/01	01/07/02	78,500	60[1]	Dual	720[2]	Bi
568RF	RAC-G	01/14/02	02/12/02	377,556	60	Dual	720	Bi
569RF	AR4000-D	03/25/03	04/11/03	217,116	60	Dual	720	Bi
571RF	45mm MB4-G	07/12/02	10/02/02	1,101,553	60	Dual	720	Bi
572RF	90mm MB4-G	01/23/03	03/12/03	537,074	60	Dual	720	Bi
573RF	MAC15-G	03/18/02	03/08/02	983,982	60	Dual	720	Bi

[1] 13,500 lb
[2] 104 psi

4.1.1 Fatigue Cracking

Digital photographs of each section taken at various time intervals during testing were processed to determine surface cracking at a given number of load applications. Figure 4.1 presents the final cracking patterns and average maximum rut depths (see Table 4.5 for definition) of each section after testing. Surface crack patterns were different for each of the HVS sections, with alligator cracks visible on Sections 567RF and 572RF; transverse cracks on Sections 568RF, 571RF, and 573RF, and a combination of alligator cracking, transverse cracking, and areas with no cracking observed on Section 569RF.

567RF (Under MB15-G) 78,500 repetitions	568RF (Under RAC-G) 377,556 repetitions	569RF (Under AR4000-D) 217,116 repetitions	571RF (Under 45mm MB4-G) 1,101,553 repetitions	572RF (Under 90mm MB4-G) 537,074 repetitions	573RF (Under MAC15-G) 983,982RF

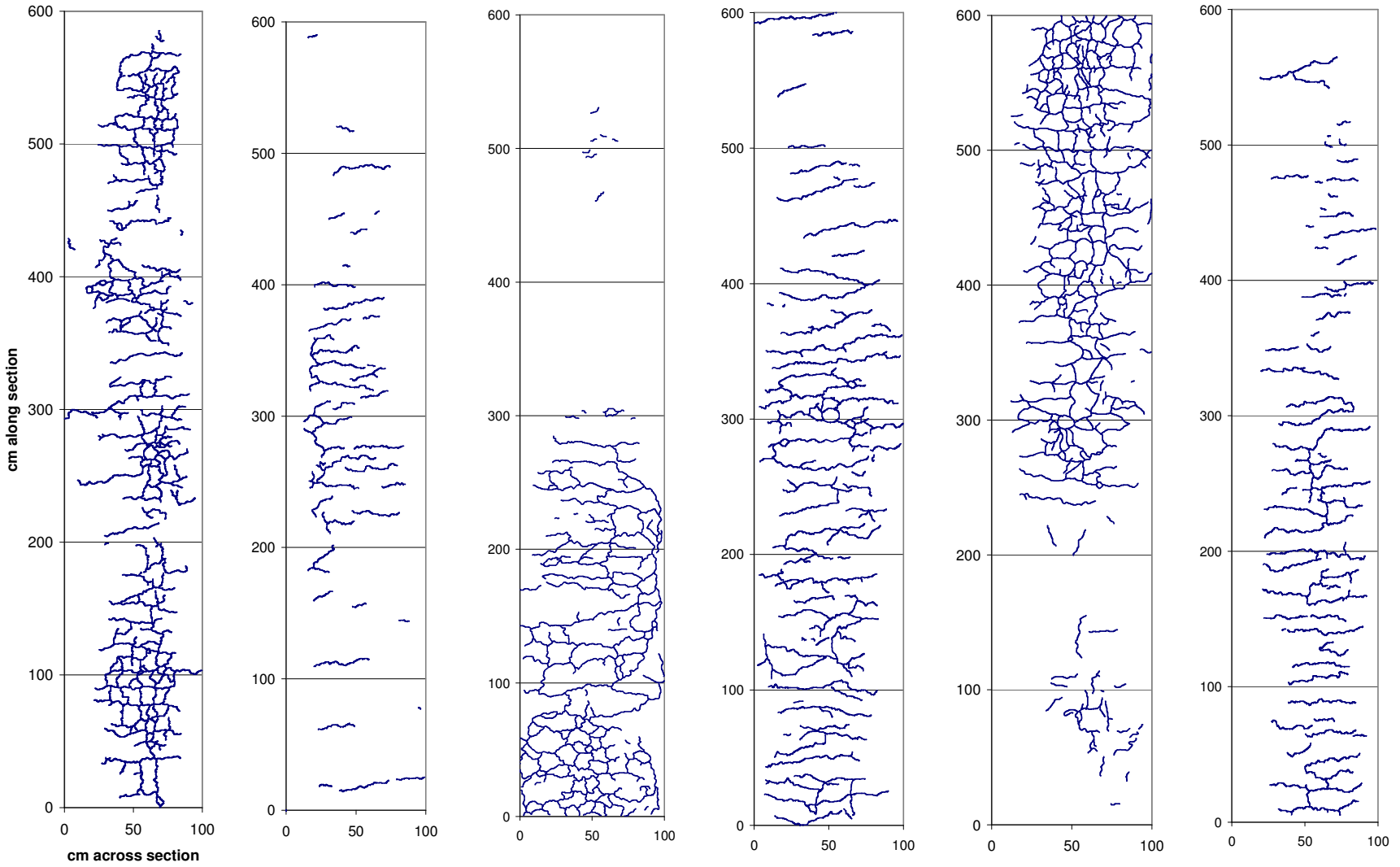

Average Maximum Rut Depths					
15.7 mm (0.62 in.)	13.9 mm (0.55 in.)	6.3 mm (0.25 in.)	14.3 mm (0.56 in.)	16.4 mm (0.65 in.)	14.6 mm (0.57 in.)

Figure 4.1: Cracking patterns and rut depths on Sections 567RF through 573RF after Phase 1.

Figure 4.2 summarizes surface cracking measurements (as crack density) with number of load applications for each Phase 1 HVS test section. HVS testing was continued beyond the 2.5 m/m^2 crack density failure criterion to assess rutting behavior and to obtain additional data for developing and calibrating performance models. Only one crack density point is shown for Sections 567RF, 569RF, and 573RF, as most cracking occurred towards the end of testing and only one set of measurements were taken. The data show much lower crack density on Sections 571RF and 573RF than on the other sections. This observation was consistent with the drier aggregate base and subgrade conditions when these sections were tested.

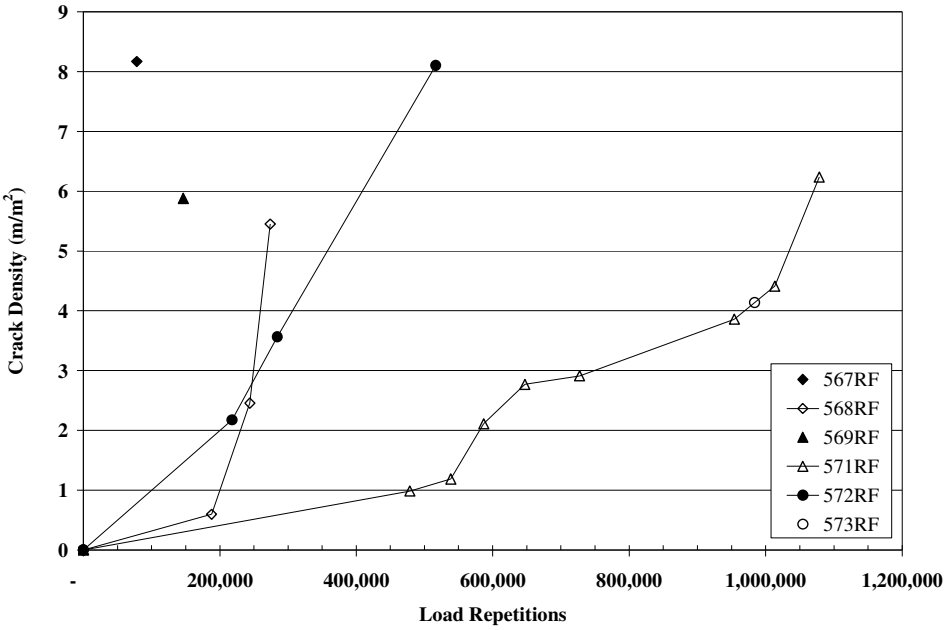

Figure 4.2: Summary of surface cracking during Phase 1.

4.1.2 Rutting

A summary of surface rutting data collected on the six Phase 1 HVS test sections is presented in Figure 4.3. HVS testing was continued beyond the 12.5-mm (0.5-in.) rutting failure criterion in order to provide more complete data for performance model development and calibration. The data showed significant variability between the HVS tests:

- Sections 571RF and 573RF had less permanent deformation and a lower rate of rutting than the other sections.
- Sections 567RF, 568RF, 569RF, and 572RF had higher rutting rates, with deepest ruts recorded on Sections 567RF and 572RF. Although the average surface rut for Section 569RF was less than 6 mm (0.24 in.), half of the section exhibited surface rutting in the range of 12 mm (0.47 in.).

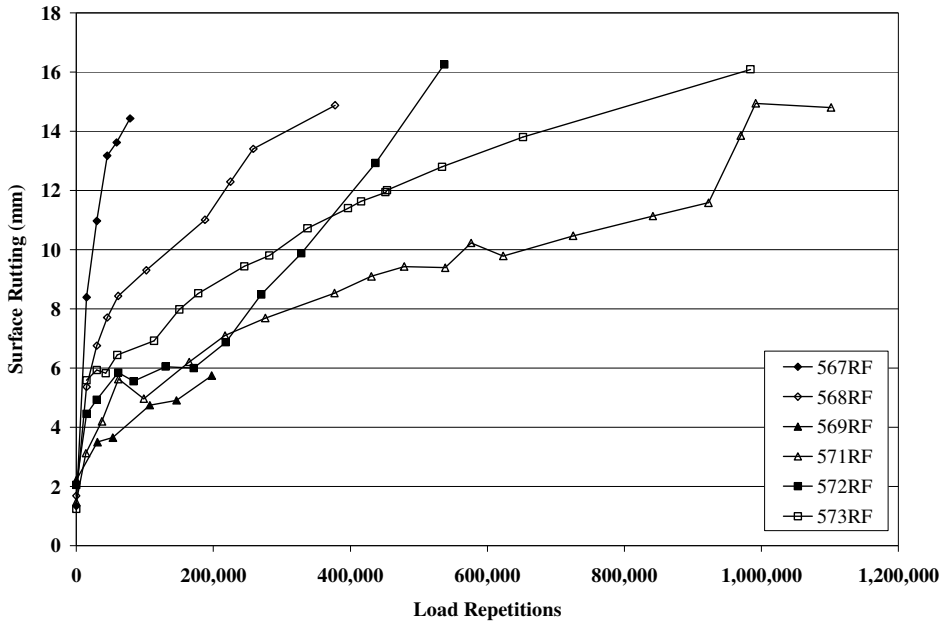

Figure 4.3: Summary of surface rutting during Phase 1.

4.2. Summary of Phase 2 HVS Testing

Phase 2 HVS rutting and reflective cracking testing is discussed in a series of first-level analysis reports (5–11), a forensic investigation report (12), and a report on the backcalculation of Falling Weight Deflectometer data collected during the course of the study (13). HVS trafficking on the six rutting sections was carried out between September 4 and December 16, 2003, and on the six reflective cracking sections between January 13, 2004 and June 25, 2007 (Table 4.2).

Table 4.2: Test Duration for Phase 2 HVS Testing

Phase	Overlay	Start Date	Finish Date	Repetitions
Rutting	MB15-G	09/29/03	10/01/03	2,000
	RAC-G	09/15/03	09/19/03	7,600
	AR4000-D	09/04/03	09/09/03	18,564
	MB4-G (45 mm)	12/08/03	12/16/03	15,000
	MB4-G (90 mm)	11/13/03	11/26/03	34,800
	MAC15-G	10/10/03	10/20/03	3,000
Reflective cracking	MB15-G	05/25/06	11/21/06	2,492,387
	RAC-G	03/15/05	10/10/05	2,024,793
	AR4000-D	11/02/05	04/11/06	1,410,000
	MB4-G (45 mm)	06/23/04	02/08/05	2,086,004
	MB4-G (90 mm)	01/13/04	06/16/04	1,981,365
	MAC15-G	01/10/07	06/25/07	2,554,335

4.2.1 Test Section Failure Criteria

Failure criteria for Phase 2 HVS testing were set as follows:

- Rutting study:
  - Maximum surface rut depth of 12.5 mm (0.5 in.) or more
- Reflective cracking study:
  - Cracking density of 2.5 m/m^2 (0.76 ft/ft^2) or more, and/or
  - Maximum surface rut depth of 12.5 mm (0.5 in.) or more.

4.2.2 Environmental Conditions

In the rutting study, the pavement surface temperature was maintained at 50°C±4°C (122°F±7°F) in order to assess the susceptibility of the mixes to early rutting under typical pavement temperatures. In the reflective cracking study, the pavement surface temperature was maintained at 20°C±4°C (68°F±7°F) for the first one million repetitions to minimize rutting in the asphalt concrete and to accelerate fatigue damage. Thereafter, the pavement surface temperature was reduced to 15°C±4°C (59°F±7°F) to further accelerate fatigue damage. A temperature control chamber was used to maintain the test temperatures. The pavement surface received no direct rainfall as it was protected by the temperature control chamber. The sections were tested during both wet and dry seasons and hence water infiltration into the pavement from the side drains and through the raised groundwater table was possible at certain stages of the testing.

4.2.3 Loading Program

The HVS loading program for each section is summarized in Table 4.3 (rutting) and Table 4.4 (reflective cracking). Test configurations were as follows:

- All trafficking was carried out with a dual-wheel configuration, using radial truck tires (Goodyear G159 - 11R22.5- steel belted radial) inflated to a pressure of 720 kPa (104 psi).
- In the rutting tests, a channelized, unidirectional loading mode was used.
- In the reflective cracking tests, a bidirectional loading mode was used and lateral wander over the one-meter width of the test section was programmed to simulate traffic wander on a typical highway lane.

Table 4.3: Loading Program for Phase 2 HVS Testing (Rutting)

Phase	Section	Start Repetition	Total Repetitions	Wheel Load (kN)[1]		ESALs	Traffic Index
				Planned	Actual[2]		
Rutting	MB15-G	Full test	2,000	40	60	11,000	N/A
	RAC-G		7,600			42,000	N/A
	AR4000-D		18,564			102,000	N/A
	45mm MB4-G		15,000			83,000	N/A
	90mm MB4-G		34,800			191,000	N/A
	MAC15-G		3,000			17,000	N/A

Table 4.4: Loading Program for Phase 2 HVS Testing (Reflective Cracking)

Phase	Section	Start Repetition	Total Repetitions	Wheel Load (kN)[1]		ESALs	Traffic Index
				Planned	Actual[2]		
Reflective cracking	MB15-G	0 215,000 410,000 1,000,001	2,492,387	40 60 80 100	60 90 80 100	88 million	15
	RAC-G	0 215,000 410,000 1,000,001	2,024,793	40 60 80 100	60 90 80 100	66 million	15
	AR4000-D	0 215,000 410,000 1,000,001	1,410,000	40 60 80 100	60 90 80 100	37 million	14
	45 mm MB4-G	0 215,000 407,197 1,002,000	2,086,004	40 60 80 100	60 90 80 100	69 million	15
	90 mm MB4-G[3]	0 1,071,004 1,439,898 1,629,058	1,981,365	40 60 80 100	60 90 80 100	37 million	14
	MAC15-G	0 215,000 410,000 1,000,001	2,554,335	40 60 80 100	60 90 80 100	91 million	15

[1] 40 kN = 9,000 lb 60 kN = 13,500 lb 80 kN = 18,000 lb 90 kN = 20,200 lb 100 kN = 22,500 lb

[2] The loading program differs from the original test plan due to an incorrect hydraulic control system setup on loads less than 65 kN in the Phase 1 experiment. The loading pattern from the Phase 1 experiment was thus retained to facilitate comparisons of performance between all tests in the Reflective Cracking Study.

[3] 590RF was the first HVS test on the overlays, and the 60 kN loading pattern was retained for an extended period to prevent excessive initial deformation (rutting) of the newly constructed overlay.

4.2.4 Rutting Study

The Phase 2 HVS rutting study was included to assess the early rutting potential of the various mixes. The tests were carried out on sections next to the demarcated reflective cracking sections on each overlay, and over a part of the underlying pavement that had not been trafficked during Phase 1. Findings and observations based on the data collected during the Phase 2 HVS rutting study include:

- An aggressive loading regime (60 kN [13,500 lb] wheel load at 50°C [122°F] pavement temperature) was followed to induce failure.
- The number of repetitions required to reach the failure criterion of 12.5 mm (0.5 in.) average maximum rut depth varied between 726 repetitions for the MAC15-G mix and 8,266 repetitions for the AR4000-D mix. Results are listed in Table 4.5, which includes ranking from best to worst, the number of load repetitions to reach an average maximum rut depth of 12.5 mm (0.5 in.), the average maximum rut depth on completion of testing, and the average deformation measured after completion of testing. The Average Maximum Rut and Average Deformation parameters are illustrated in the figure below the table. The ranking is shown graphically in Figure 4.4.

Table 4.5: Phase 2 Rutting Study Results

Overlay	Rank	Repetitions to 12.5 mm (0.5 in.) Average Maximum Rut*	Average Maximum Rut (mm [in.])	Average Deformation (mm [in.])
AR4000-D	1	8,266	15.6 (0.6)	8.1 (0.3)
MB4-G (45 mm)	2	3,043	31.3 (1.3)	9.7 (0.4)
RAC-G	3	2,324	22.7 (0.9)	10.3 (0.4)
MB4-G (90 mm)	4	1,522	23.3 (0.9)	11.9 (0.5)
MB15-G	5	914	18.8 (0.8)	7.1 (0.3)
MAC15-G	6	726	23.5 (0.9)	7.7 (0.3)

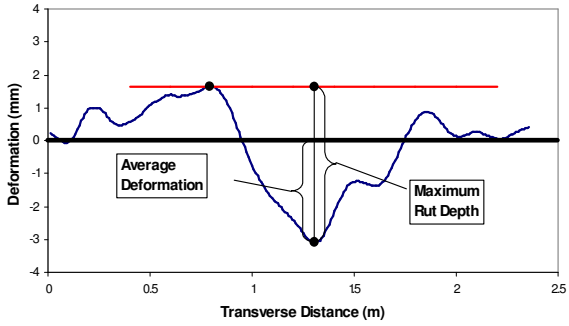

* The average maximum rut is the mean of the maximum rut depths measured at each measuring station between Stations 2 and 14 as shown on Figure 3.7

- Analysis of surface profiles and test pit observations during a forensic investigation (12) indicate that most of the permanent deformation occurred in the underlying DGAC surfacing layer (Figure 4.5). The deformation along each section was reasonably uniform, with the exception of the 90-mm MB4-G, where more severe rutting and heaving occurred at one end of the test section compared to the other. All of the sections showed some heaving at the sides of the trafficked area, with heights varying between 5 mm (0.2 in.) and 16 mm (0.6 in.).

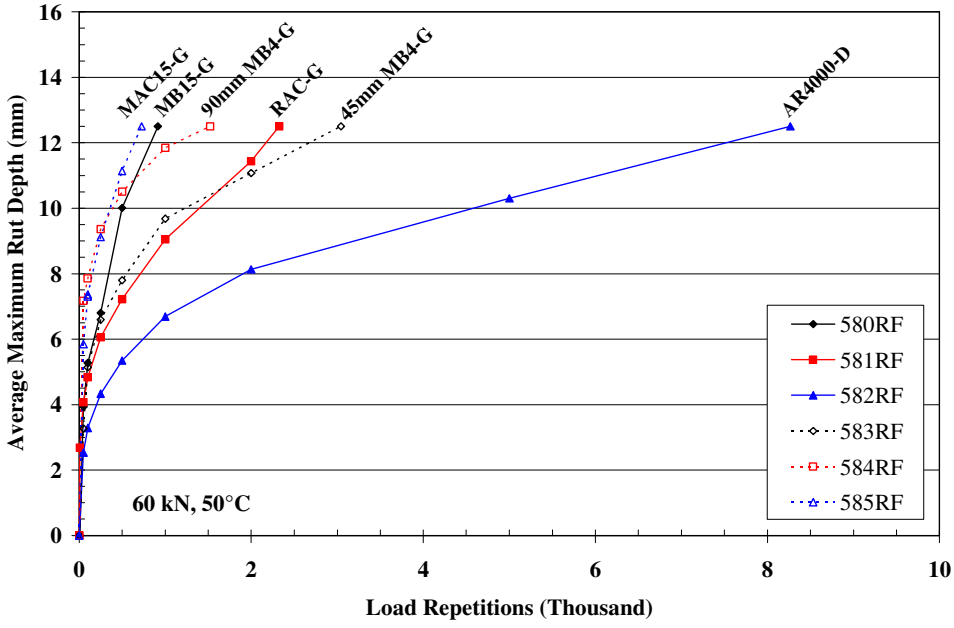

Figure 4.4: Progression of average maximum rut depth to 12.5 mm (0.5 in.) failure criteria.

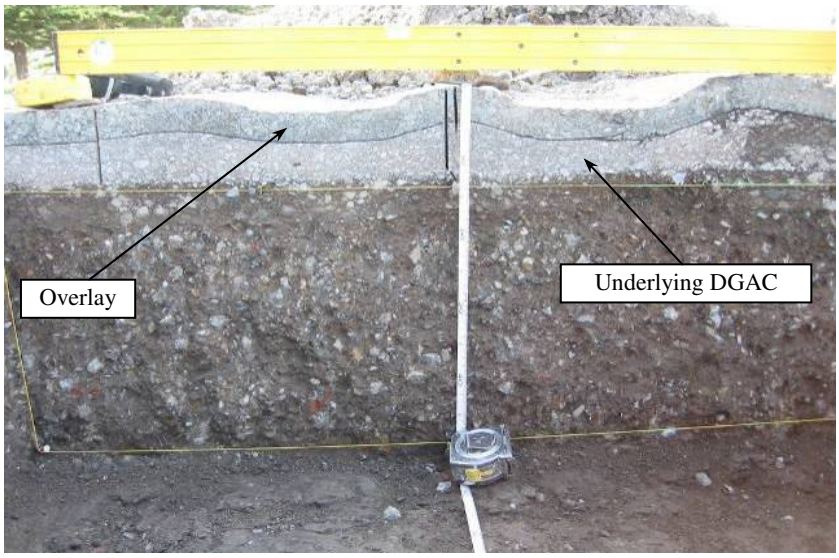

Figure 4.5: Rutting in the underlying DGAC on the 45-mm MB4-G section.

4.2.5 Reflective Cracking Study

A summary of the findings from each HVS test, in the order undertaken, is provided below.

Section 590RF: 90 mm MB4-G

Section 590RF was the first HVS test on the overlays, and the 60 kN loading pattern was retained for an extended period to prevent excessive initial deformation (rutting) of the newly constructed overlay. Once rutting behavior was better understood, the load was increased. The loading program for the remaining five sections was revised based on these observations (see Table 4.3). A total of almost 2.0 million repetitions were applied. Findings and observations based on the data collected during this HVS study include:

- No cracking was observed on the MB4-G overlay after almost two million HVS repetitions. The MB4-G overlay thus appeared to successfully prevent any cracking in the underlying layer from reflecting through to the surface, despite final-to-initial deflections indicating that considerable damage had occurred in the asphalt layers under loading.
- The average maximum rut depth across the entire test section at the end of the test was 12.7 mm (0.5 in.), approximately equivalent to the Caltrans (and experiment) failure criterion. The maximum rut depth measured on the section was 19.0 mm (0.7 in.), with a maximum rut depth of 12.5 mm reached after about 1.17 million repetitions, soon after the load increase from 60 kN (13,500 lb) to 90 kN (20,250 lb).
- Ratios of final-to-initial elastic surface deflections (i.e. comparison of deflections at the end of the test with those at the beginning of the test) under a 60 kN (13,500 lb) wheel load increased by between 1.9 and 3.0 times along the length of the section. The ratios for in-depth deflections

show that damage increased at all depths in the pavement structure (between 1.9 and 2.2 times) by the end of trafficking. Loss of stiffness was highest in the area of most severe cracking in the underlying DGAC layer.

- Analysis of surface profile and in-depth permanent deformation measurements indicates that most of the permanent deformation (between 67 and 88 percent) occurred in the asphalt-bound surfacing layers (overlay and underlying DGAC) with marginal deformation in the base layer and negligible deformation in the subgrade. These findings were confirmed in the forensic investigation.

Section 589RF: 45 mm MB4-G

A total of almost 2.1 million repetitions were applied during this HVS test. Findings and observations based on the data collected include:

- Some cracking was observed after about 1.5 million repetitions at one end of the section where significant deformation (rutting and shoving) had occurred. No further cracking was noted after about 1.6 million repetitions. On completion of testing, the crack density was 1.55 m/m^2 (0.47 ft/ft^2), considerably lower than the failure criterion of 2.5 m/m^2 (0.76 ft/ft^2) set for the experiment. The cracks were predominantly longitudinal and cracking patterns did not correspond with those in the underlying DGAC layer. Apart from the cracks associated with deformation at the end of the section, the MB4-G overlay appeared to successfully prevent any cracking in the underlying layer from reflecting through to the surface, despite final-to-initial deflections indicating that considerable damage had occurred in the asphalt layers.
- The average maximum rut depth across the entire test section at the end of the test was 37.2 mm, (1.46 in.) which exceeded the Caltrans (and experiment) failure criterion of 12.5 mm (0.5 in.) reached after approximately 820,000 repetitions. At this point, no cracking was observed and the test was therefore continued to gain a better understanding of the MB4-G overlay performance. The maximum rut depth measured on the section at the end of the test was 106 mm (4.17 in.). Despite conducting HVS testing at relatively low pavement temperatures (20°C [68°F]) for the first one million repetitions and 15°C [59°F] for the remainder of the test), the MB4-G overlay appeared susceptible to rutting from early in the experiment.
- Ratios of final-to-initial elastic surface deflections under a 60 kN (13,500 lb) wheel load increased by between 2.1 and 2.9 times along the length of the section. The ratios for in-depth deflections show that damage had increased significantly at all depths in the pavement structure by the end of trafficking. Loss of stiffness was highest in the area of most severe cracking in the underlying DGAC layer.

- Analysis of surface profile and in-depth permanent deformation measurements indicate that most of the permanent deformation (between 68 and 86 percent along the length of the section) occurred in the asphalt-bound surfacing layers (overlay and underlying DGAC) with the remainder in the aggregate base layer. Some deformation occurred in the subgrade below the point of greatest maximum rut. Contribution to total permanent deformation at this point was 68, 26, and 6 percent for the surfacing, aggregate base, and subgrade respectively. These findings were confirmed in the forensic investigation.

Section 587RF: RAC-G

Slightly more than two million repetitions were applied during this HVS test. Findings and observations based on the data collected include:

- Cracking was first observed after approximately 1.5 million repetitions. On completion of testing, the surface crack density was 3.6 m/m^2 (1.10 ft/ft^2), considerably lower than the 5.4 m/m^2 (1.65 ft/ft^2) recorded after 377,556 repetitions on the underlying layer during Phase 1 HVS trafficking. The surface crack density reached 2.5 m/m^2 (0.76 ft/ft^2), the failure criterion set for the experiment, after about 1.9 million load repetitions. Cracking on the overlay was predominantly transverse, as was that on the underlying layer. The crack patterns of the two layers did not match exactly; however, the areas of most severe cracking corresponded (Figure 4.6).

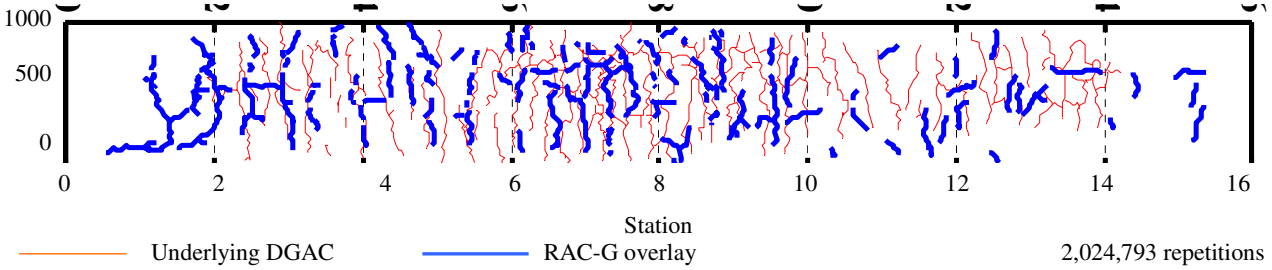

Figure 4.6: Cracking pattern comparison between underlying layer and RAC-G overlay.

- The average maximum rut depth across the entire test section at the end of the test was 18.2 mm (0.7 in.), which was higher than the failure criterion of 12.5 mm (0.5 in.) set for the experiment, reached after approximately 1.8 million repetitions. The maximum rut depth measured on the section was 26.3 mm (1.1 in.). The rate of rutting was relatively slow during the early part of the experiment, but increased significantly after the 100 kN (22,500 lb) load change, despite the pavement temperature being reduced to 15°C (59°F).
- Both failure criteria set for the experiment were reached within 100,000 load repetitions of each other.

- Ratios of final-to-initial elastic surface deflections under a 60 kN (13,500 kN) wheel load increased by between 3.4 and 5.5 times along the length of the section. The ratios for in-depth deflections show that damage had increased significantly at all depths in the pavement structure by the end of trafficking. The limited data available shows that loss of stiffness in the section was highest in the area of most severe cracking in the underlying layer.
- Analysis of surface profile and in-depth permanent deformation measurements indicate that most of the permanent deformation occurred in the asphalt-bound surfacing layers (overlay and underlying DGAC) with approximately twice as much damage occurring in the area of most severe cracking in the underlying DGAC layer. Permanent deformation was also recorded in the upper part of the aggregate base in this area. Negligible deformation was recorded in the subgrade. These findings were confirmed in the forensic investigation.

Section 588RF: AR4000-D

Approximately 1.4 million repetitions were applied during this HVS test. Findings and observations based on the data collected include:

- Cracking was first observed after approximately 510,000 repetitions. On completion of testing, the surface crack density was 9.1 m/m^2 (2.77 ft/ft^2), with cracking occurring predominantly on one half of the section (Stations 8 to 15 [see Figure 3.7]). The surface crack density reached 2.5 m/m^2 (0.76 ft/ft^2), the failure criterion set for the experiment, after about 900,000 load repetitions, but trafficking was continued to determine whether cracking would eventually spread to the remainder of the test section. Cracking on the overlay was predominantly transverse up until the 100 kN (22,500 lb) load change. Thereafter, an alligator cracking pattern was observed, similar to that on the underlying layer. The crack patterns of the two layers did not match exactly; however, the areas of most severe cracking corresponded (Figure 4.7).

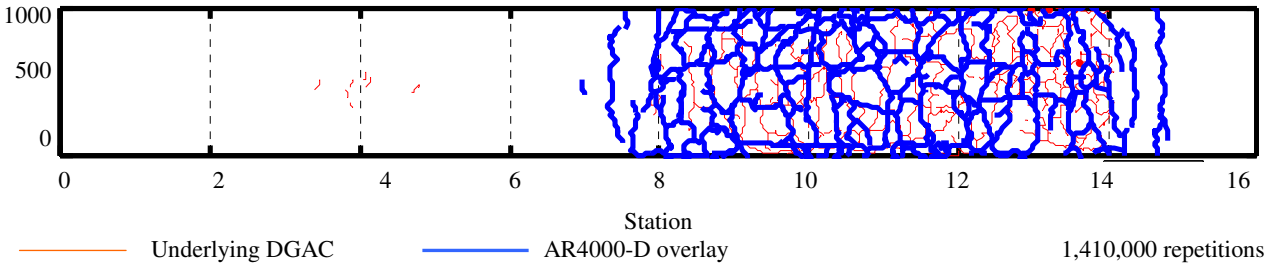

Figure 4.7: Cracking pattern comparison between underlying layer and AR4000-D overlay.

- The average maximum rut depth and average maximum deformation across the entire test section at the end of the test was 15.9 mm (0.63 in.) and 8.8 mm (0.35 in.) respectively. The average maximum rut was higher than the failure criterion of 12.5 mm (0.5 in.) set for the experiment,

reached after approximately 1.2 million repetitions. As indicated above, testing was continued to determine whether cracking would eventually spread to the remainder of the test section. The maximum rut depth measured on the section was 30 mm (1.18 in.). The rate of rutting was relatively slow during the early part of the experiment, but increased significantly after the 100 kN (22,500 lb) load change, despite the pavement temperature being reduced to 15°C (59°F). The final surface rutting pattern of the overlay generally corresponds with the fatigue cracking pattern, and the deepest part of the rut occurred on that half of the section with the highest density of cracking in the underlying DGAC layer.

- The two failure criteria set for the experiment were reached within approximately 300,000 load repetitions of each other.
- Ratios of final-to-initial elastic surface deflections under a 60 kN (13,500 lb) wheel load increased by between 4 and 11 times along the length of the section, indicating significant damage in the pavement structure in terms of loss of stiffness. The ratio of final-to-initial deflections was inconsistent across the section, with significantly higher values in the area overlying the most severely cracked area.
- No in-depth elastic deflection or permanent deformation data were collected in this experiment due to problems with the Multi-Depth Deflectometers (MDDs). Malfunction was attributed to the loss of anchorage of the modules resulting from very wet conditions in the lower layers of the pavement and subgrade. Subsequent forensic investigations indicate that most of the permanent deformation occurred in the asphalt-bound surfacing layers (overlay and underlying DGAC) with approximately twice as much damage occurring in the area of most severe cracking in the underlying DGAC layer.
- Parts of the test were carried out during relatively high rainfall. This resulted in ponding of water adjacent to the section. Some pumping of fines through the cracks was noted in the final days of testing.

Section 586RF: MB15-G

The failure criteria set for the test was not reached after 2.5 million repetitions. Given time and fund limitations in the study, Caltrans and the UCPRC agreed to halt the test at this point. Findings and observations based on the data collected during this HVS study include:

- The MB15-G overlay appeared to successfully prevent any cracking in the underlying layer from reflecting through to the surface, despite final-to-initial deflections indicating that damage had occurred in the asphalt layers under loading.
- The average maximum rut depth across the entire test section at the end of the test was just 4.6 mm (0.2 in.), considerably lower than the Caltrans (and experiment) failure criterion of

12.5 mm (0.5 in.). The maximum rut depth measured on the section was 7.7 mm (0.3 in.). The MB15-G overlay thus did not appear susceptible to rutting in the temperature range at which the test was conducted (20°C [68°F] for the first one million repetitions and 15°C [59°F] thereafter).

- Ratios of final-to-initial elastic surface deflections under a 60 kN (13,500 lb) wheel load increased by between 1.4 and 1.9 times along the length of the section. The ratios for in-depth deflections show that damage increased at all depths in the pavement structure by the end of trafficking. Loss of stiffness was highest in the area of most severe cracking in the underlying DGAC layer.
- Analysis of surface profile and in-depth permanent deformation measurements indicated that most of the permanent deformation (approximately 55 percent) occurred in the asphalt-bound surfacing layers (overlay and underlying DGAC) with the remainder mostly in the aggregate base layer. These findings were confirmed in the forensic investigation. After the first one million repetitions had been applied, the permanent deformation in the surfacing layers was higher (approximately 70 percent).

Section 591RF: MAC15-G

The failure criteria set for the test was not reached after 2.5 million repetitions. Given time and fund limitations for the study, Caltrans and the UCPRC agreed to halt the experiment at this point. Findings and observations based on the data collected during this HVS study include:

- The MAC15-G overlay appeared to successfully prevent any cracking in the underlying layer from reflecting through to the surface, despite final-to-initial deflections indicating that damage had occurred in the asphalt layers under loading.
- The average deformation and average maximum rut depth across the entire test section at the end of the test was just 1.7 mm (0.1 in.) and 4.6 mm (0.2 in.) respectively, with average maximum rut considerably lower than the Caltrans (and experiment) failure criterion of 12.5 mm (0.5 in.). The maximum rut depth measured on the section was 8.2 mm (0.3 in.). The MAC15-G overlay thus did not appear susceptible to rutting in the temperature range at which the test was conducted (20°C [68°F] for the first one million repetitions and 15°C [59°F] thereafter).
- Ratios of final-to-initial elastic surface deflections under a 60 kN (13,500 lb) wheel load increased by between 3.7 and 4.0 times along the length of the section. The ratios for in-depth deflections show that damage increased at all depths in the pavement structure by the end of trafficking. Loss of stiffness was highest in the area of most severe cracking in the underlying DGAC layer.
- Analysis of surface profile and in-depth permanent deformation measurements indicates that most of the permanent deformation (between 55 and 60 percent) occurred in the asphalt-bound surfacing layers (overlay and cracked DGAC) with the remainder mostly in the aggregate base layer. These findings were confirmed in the forensic investigation. After the first one million

repetitions had been applied, the permanent deformation in the surfacing layers was higher (between 80 and 90 percent).

Phase 2 Cracking Patterns

Figure 4.8 presents the final cracking patterns of each section after Phase 2 HVS testing.

4.3. Forensic Investigation

A total of 18 test pits were excavated as part of a forensic investigation on the Phase 2 HVS test sections. This included one test pit on each rutting section (between Stations 6 and 8 [see Figure 3.7]) and two test pits on each reflective cracking section (between Stations 4 and 6 and between Stations 10 and 12). The pits were excavated approximately 200 mm (8 in.) into the subgrade below the base. The wet density of the base material in each pit was measured with a nuclear density gauge and in situ shear strength of the base and subgrade material was measured with a Dynamic Cone Penetrometer (DCP) in the test section wheelpath as well as in an untrafficked area. Findings and observations based on the data collected during this forensic investigation include:

- There was considerable variation in the thicknesses of the base, underlying DGAC, and the overlays over the length and width of the test road.
- In the rutting experiments, rutting occurred primarily in the underlying DGAC and not in the overlay (Figure 4.5). On the reflective cracking experiments, rutting occurred in both layers. Rutting from the Phase 1 trafficking was clearly visible on most test pit profiles (Figure 4.9). Very little rutting occurred in the base and no rutting was recorded in the subgrade. This corresponds to the Multi-Depth Deflectometer permanent deformation analyses discussed in the first-level reports on each section.

MB15-G 2,492,387 repetitions	RAC-G 2,024,793 repetitions	AR4000-D 1,410,000 repetitions	45mm MB4-G 2,086,004 repetitions	90mm MB4-G 1,981,365 repetitions	MAC15-G 2,554,335 repetitions
No cracking at completion of HVS testing	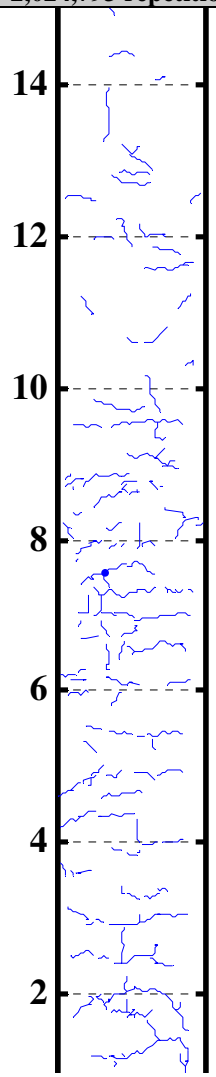	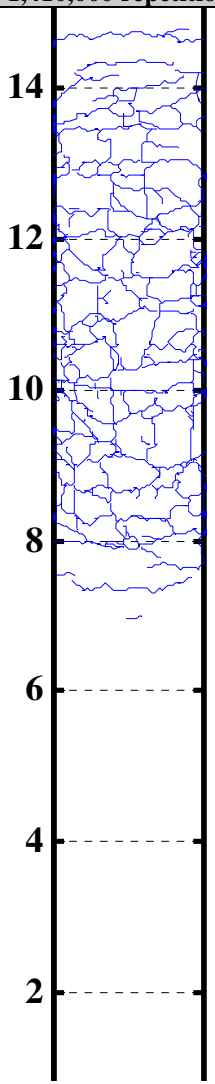	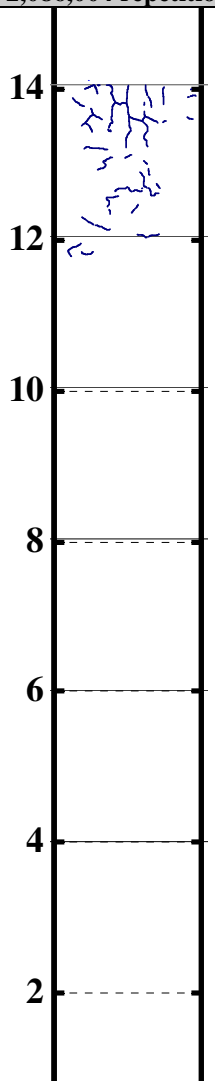	No cracking at completion of HVS testing	No cracking at completion of HVS testing
Average Maximum Rut Depths					
4.6 mm (0.18 in.)	18.2 mm (0.72 in.)	15.9 mm (0.63 in.)	37.2 mm (1.46 in.)	12.7 mm (0.5 in.)	1.7 mm (0.07 in.)

Figure 4.8: Cracking patterns and rut depths on Sections 586RF through 591RF after Phase 2.

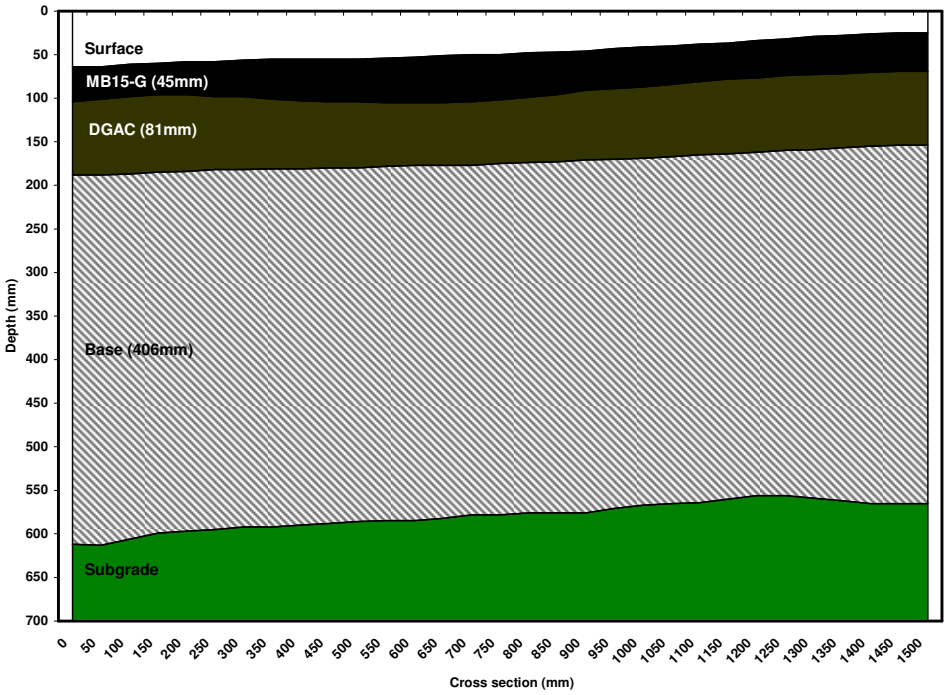

Figure 4.9: Test pit profile showing rutting from Phase 1 HVS testing (MB15-G section).

- Cracks were observed on some of the test pit profiles (Figure 4.10). In the underlying DGAC layer, cracks were generally clearly visible. However, in the modified binder overlays, heat generated from the saw cut operation appeared to seal any cracks and no conclusions could be drawn as to the depth that cracks had reflected into the overlays. Most cracks (that could be traced) appeared to have initiated close to the bottom of the underlying DGAC. Some crack initiation was also observed at poorly bonded joints between lifts and overlays in the AR4000-D section. No additional information was gathered from an assessment of cores. No cracking was observed in the base.

Figure 4.10: Test pit profile showing highlighted cracks (RAC-G section).

- Some post-construction cementation of the base material appeared to have occurred. This was substantiated with Dynamic Cone Penetrometer (DCP) tests, close inspection of the test pit profile, the use of phenolphthalein to determine the pH of the base material, and examination of specimens under optical and scanning electron microscopes. This recementation appears to have contributed to the good performance of the sections.
- Densities were generally consistent throughout the section. Nuclear gauge-determined wet densities averaged 2,176 kg/m^3 (standard deviation of 34 kg/m^3 [135.8 pcf, standard deviation of 2.1 pcf), which corresponds with the average wet density of 2,200 kg/m^3 (137.3 pcf) for the road base recorded after construction.
- Nuclear gauge-determined moisture contents averaged 11.1 percent (standard deviation of 1.1 percent) for the eighteen test pits. In most test pits, the moisture content in the upper 50 mm (2 in.) was on the order of one percent higher than in the material between 150 mm (6 in.) and 200 mm (8 in.). The optimum moisture content of the Class 2 aggregate base material, determined prior to construction, was 8.9 percent, somewhat lower than the average recorded with the nuclear gauge. Laboratory-determined gravimetric moisture contents averaged 8.7 percent, which was closer to the optimum moisture content.
- Subgrade densities were not measured. The average subgrade moisture content was 15 percent (lowest of 12.9 percent and highest of 18.0 percent), considerably higher than the base moisture content. The presence of mottling in the subgrade material indicated that the moisture content probably fluctuated seasonally.
- The air-void contents of cores removed from the wheelpaths in the reflective cracking sections after HVS testing were generally lower compared to those determined from cores removed from outside the sections prior to HVS testing, as expected.

4.4. Reports

The following reports were prepared for this phase of the study:

- BEJARANO, M., Jones, D., Morton, B., and Scheffy, C. 2005. **Reflective Cracking Study: Summary of Construction Activities, Phase 1 HVS Testing, and Overlay Construction**. Davis and Berkeley, CA: University of California Pavement Research Center. (UCPRC-RR-2005-03).
- JONES, D., Tsai, B.W., and Harvey, J. 2006. **Reflective Cracking Study: First-level Report on HVS Testing on Section 590RF — 90 mm MB4-G Overlay.** Davis and Berkeley, CA: University of California Pavement Research Center. (UCPRC-RR-2006-04).

- JONES, D., Wu, R., Lea, J., and Harvey, J. 2006. **Reflective Cracking Study: First-level Report on HVS Testing on Section 589RF — 45 mm MB4-G Overlay.** Davis and Berkeley, CA: University of California Pavement Research Center. (UCPRC-RR-2006-05).
- WU, R., Jones, D., and Harvey, J. 2006. **Reflective Cracking Study: First-level Report on HVS Testing on Section 587RF — 45 mm RAC-G Overlay.** Davis and Berkeley, CA: University of California Pavement Research Center. (UCPRC-RR-2006-06).
- JONES, D., Wu, R., and Harvey, J. 2006. **Reflective Cracking Study: First-level Report on HVS Testing on Section 588RF — 90 mm DGAC Overlay.** Davis and Berkeley, CA: University of California Pavement Research Center. (UCPRC-RR-2006-07).
- JONES, D., Wu, R., and Harvey, J. 2006. **Reflective Cracking Study: First-level Report on HVS Testing on Section 586RF — 45 mm MB15-G Overlay.** Davis and Berkeley, CA: University of California Pavement Research Center. (UCPRC-RR-2006-12).
- JONES, D., Wu, R., and Harvey, J. 2007. **Reflective Cracking Study: First-level Report on HVS Testing on Section 591RF — 45 mm MAC15-G Overlay.** Davis and Berkeley, CA: University of California Pavement Research Center. (UCPRC-RR-2007-04).
- STEVEN, B., Jones, D., and Harvey, J. 2007. **Reflective Cracking Study: First-level Report on the HVS Rutting Experiment.** Davis and Berkeley, CA: University of California Pavement Research Center. (UCPRC-RR-2007-06).
- LU, Q., Jones, D., and Harvey, J. 2007. **Reflective Cracking Study: Backcalculation of HVS Test Section Deflection Measurements.** Davis and Berkeley, CA: University of California Pavement Research Center. (UCPRC-RR-2007-04).
- JONES, D., Harvey, J., and Steven, B. 2007. **Reflective Cracking Study: HVS Test Section Forensic Report.** Davis and Berkeley, CA: University of California Pavement Research Center. (UCPRC-RR-2007-05).

5. LABORATORY FATIGUE AND SHEAR TESTING

Laboratory fatigue (flexural beam) and shear testing (repeated simple shear at constant height) was carried out to obtain an understanding of the performance and behavior of the various mixes under controlled conditions for later comparison with HVS test results, and mechanistic-empirical analyses of HVS and in-service performance. Fatigue testing was carried out on specimens prepared from loose mix collected from the paver during construction, and from aggregate and binder samples collected at the asphalt plant. Shear testing was carried out on similar specimens, as well as on cores removed from the test track. Findings were presented in two first-level reports.

5.1. Laboratory Fatigue

5.1.1 Sampling

Laboratory fatigue testing was carried out on beams cut from slabs prepared using rolling wheel compaction. Materials used to prepare the slabs were sampled from:

- Loose mix collected from the paver during construction, referred to in the report as field-mixed, laboratory-compacted (FMLC) samples, and
- Stockpiles at the asphalt plant, referred to in the report as laboratory-mixed, laboratory-compacted (LMLC) samples.

5.1.2 Test Protocols

The laboratory fatigue study followed the AASHTO T321 test procedures (developed by the Strategic Highway Research Program [SHRP] A-003A project), which consist of flexural controlled-deformation fatigue tests and frequency sweep tests.

5.1.3 Experiment Design

The experiment design was formulated to quantify the effects of:

- Temperature,
- Relative compaction (air voids),
- Aging, and
- Gradation.

In order to test a full factorial, a total of 1,440 tests (three replicates of five binder types, two compaction types, two condition types, two gradations, two air-void contents, three temperatures, and two strain levels) would need to have been undertaken. This quantity was unrealistic in terms of time and resources. A partial factorial consisting of 256 tests was therefore tested, and where possible the same tests under different effects were not repeated. Results were extrapolated where required.

5.1.4 Findings and Observations

Summary of Binder Tests

- Based on Bending Beam Rheometer (BBR) test results conducted by the Federal Highway Administration (FHWA), the ranking of propensity to low-temperature thermal cracking is listed below, from best to worst. The RAC binder was not tested due to limitations of the equipment used with respect to crumb rubber.
    1. MB4
    2. MB15
    3. MAC15
    4. AR4000
- The order of thermal cracking potential was closely matched by the order of initial stiffness in the fatigue beam tests and flexural frequency sweep results; hence a mix with a higher initial stiffness might have a higher thermal cracking potential.
- The Dynamic Shear Rheometer (DSR) test results indicated that:
    - The MAC15 binder did not meet the Superpave rutting specification at any test temperature.
    - The MB4 and MB15 binders had better rutting resistance capacities than the AR4000 binder.
    - According to the Superpave specification, the ranking of fatigue resistance capacity was in the order listed below (best to worst), which is the same ranking obtained for initial stiffness during laboratory mix fatigue tests.
        1. MB4
        2. MB15
        3. MAC15
        4. AR4000

Test Effects

- The binder type had an overall effect on all the response variables including initial phase angle, initial stiffness, and fatigue life. As expected, the temperature effect on all three response

variables was immediately apparent. The other effects assessed at 20°C (68°F, for comparison with HVS testing) revealed that:

- Air-void content had a significant effect for some parts of the experiment, such as the FMLC mixes at 20°C, but the effect was not significant for many of the mixes and test conditions for all of the response variables.
- The aging effect was only significant for initial phase angle and stiffness but not for fatigue life.
- All the response variables were significantly affected by the change from a gap-gradation to a dense-gradation for the MAC15-G, MB15-G, and MB4-G mixes.

Ranking of Initial Stiffness and Fatigue Performance

- The ranking of predicted initial stiffness and fatigue life under various specimen preparation and testing conditions, and specifically for the controlled strain mode of loading used in this experiment, was normally in the order listed below. For initial stiffness, no apparent differences existed between the MB15-G and MB4-G mixes, while for fatigue life, no apparent differences existed between the MAC15-G and MB15-G mixes. As expected, the two orders are reversed.

Initial Stiffness	Beam Fatigue Life
1. AR4000-D	1. MB4-G
2. RAC-G	2. MAC15-G and MB15-G
3. MAC15-G	4. RAC-G
4. MB15-G and MB4-G	5. AR4000-D

- Fatigue test results indicated that initial stiffness and fatigue life were moderately negative-correlated (ρ = -0.604), confirming a general observation that lower stiffnesses equate to higher fatigue life at a given tensile strain under controlled-strain testing when ranking fatigue life performance against initial stiffness or vice versa. However, when using this observation, consideration must also be given to rutting, as mixes with low stiffness are generally susceptible to this distress.
- Preliminary analysis of stiffness-versus-strain repetition curves using three-stage Weibull analysis indicated differences in crack initiation and propagation. The AR4000-D mix had different behavior from that of the RAC-G mix, while the RAC-G mix performed differently than the MB4-G, MB15-G, and MAC15-G mixes. The results indicate that damage may slow during the propagation phase of the latter four mixes, while it accelerates for the AR4000-D mix.

Dense-Graded versus Gap-Graded Mixes (Laboratory-Mix, Laboratory-Compacted)

- The optimum binder contents used in the mix designs for the MAC15, MB15, and MB4 dense-graded mixes (6.0, 6.0, and 6.3 percent respectively) were lower than the optimum binder contents used in the mix designs of the gap-graded mixes (7.4, 7.1, and 7.2 percent respectively).
- Limited fatigue testing of modified binders in dense-graded mixes led to the following observations:
    - The initial stiffnesses of the dense-graded modified-binder mixes were generally greater than those of the corresponding gap-graded mixes but less than those of the AR4000-D and RAC-G mixes.
    - The beam fatigue lives at a given tensile strain of the dense-graded mixes were generally less than those of the corresponding gap-graded mixes, but greater than those of the AR4000-D and RAC-G mixes.
    - The mix ranking of initial stiffness, from most to least stiff, for laboratory mixed, laboratory compacted specimens at 6 percent air-voids was:
        1. AR4000-D
        2. MAC15-D
        3. RAC-G
        4. MB15-D
        5. MB4-D
        6. MAC15-G
        7. MB15-G
        8. MB4-G
    - The mix ranking for the same conditions for beam fatigue life at 400 microstrain showed exactly the reverse trend from the above except that MAC15-D and RAC-G changed places:
        1. MAC15-G
        2. MB4-G
        3. MB15-G
        4. MB4-D
        5. MB15-D
        6. MAC15-D
        7. RAC-G
        8. AR4000-D

Complex Modulus Master Curves of Mixes (Laboratory-Mixed, Laboratory-Compacted)

- Complex modulus master curves from flexural frequency sweep tests showed mix stiffnesses for a wide range of temperature and time of loading conditions. Initial stiffnesses determined from beam fatigue tests were only for 10 Hz and the temperature at which the fatigue test was performed. However, the mix ranking of the complex modulus master curves under various combinations of material properties and testing conditions was generally in the order listed below,

and is comparable to the overall general ranking of beam fatigue performance in the controlled-strain testing. The MB4-G and MB15-G mixes showed no significant difference in master curves.

Master Curve Stiffness	Beam Fatigue Life
1. AR4000-D	1. MB4-G and MB15-G
2. RAC-G	3. MAC15-G
3. MAC15-G	4. RAC-G
4. MB15-G	5. AR4000-D
5. MB4-G	

- The ranking of complex modulus master curves for dense-graded mixes considering the effect of gradation was in the order below, with no significant difference between the MB4-D and MB15-D mixes:
    1. MAC15-D
    2. MB4-D
    3. MB15-D

5.2. Laboratory Shear

5.2.1 Sampling

Laboratory shear testing was carried out on cores removed from the test track, next to the demarcated HVS test sections (referred to as field-mixed, field-compacted [FMFC] samples in the report), and cores prepared with materials sampled from:

- Loose mix collected from the paver during construction, referred to as field-mixed, laboratory-compacted (FMLC) samples in the report, and
- Stockpiles at the asphalt plant, referred to as laboratory-mixed, laboratory-compacted (LMLC) samples in the report.

Cores were cut from slabs prepared using rolling wheel compaction.

5.2.2 Test Protocols

The laboratory fatigue study followed the AASHTO T320 test procedures, *Determining the Permanent Shear Strain and Stiffness of Asphalt Mixtures Using the Superpave Shear Tester (SST), Procedure C, Repeated Shear Test at Constant Height*, developed by the Strategic Highway Research Program (SHRP).

5.2.3 Experiment Design

The experiment design was formulated to quantify the effects of:

- Applied shear stress,
- Temperature,
- Degree of compaction (air voids),
- Mix aging,
- Mixing and compaction method, and
- Aggregate gradation.

In order to test a full factorial, a total of 2,880 tests (three replicates of five binder types, two mix types, two compaction types, two condition types, two gradations, two air-void contents, two temperatures, and three stress levels) would need to have been undertaken. This quantity was unrealistic in terms of time and resources. Therefore, a partial factorial consisting of 227 tests was tested, and where possible, the same tests under different effects were not repeated. Results were extrapolated where required.

5.2.4 Findings and Observations

Overall Summary of Repeated Simple Shear Test Results

- The binder type had an overall effect on all the response variables including Permanent Shear Strain (PSS) at 5,000 Cycles, Cycles to 5 Percent Permanent Shear Strain, and Shear Stiffness (resilient shear modulus [G^*]). As expected, the temperature effect on all three response variables was immediately apparent and significant. The other effects assessed (for comparison with HVS testing) revealed that:
    - Air-void content had a significant effect for Cycles to 5 Percent Permanent Shear Strain and Permanent Shear Strain at 5,000 Cycles but the effect was not significant for Shear Stiffness.
    - Overall, the long-term aging effect was only minimally significant.
    - For MAC15, MB15, and MB4 mixes, all the response variables were significantly affected by the change from a gap gradation to a dense gradation. As expected, rutting performance improved when the binders were used with the dense gradation as opposed to gap gradation.

Performance Ranking

The ranking of the Cycles to 5 Percent Permanent Shear Strain (5% PSS), Permanent Shear Strain at 5,000 Cycles (PSS@5000 Cycles), and Shear Stiffness (resilient shear modulus) parameters under the various

specimen preparation and testing conditions for the shear test used in this study is listed below from best to worst with respect to expected rutting performance.

Cycles to 5% PSS	PSS at 5,000 Cycles	Resilient Shear Modulus (G^*)
1. AR4000-D	1. AR4000-D	1. AR4000-D
2. MAC15-G	2. MAC15-G	2. RAC-G
3. RAC-G	3. RAC-G	3. MAC15-G
4. MB4-G	4. MB4-G	4. MB4-G
5. MB15-G	5. MB15-G	5. MB15-G

Dense-Graded versus Gap-Graded Mixes

- The optimum binder contents used in the mix designs based on Hveem stabilometer tests for the MAC15, MB15, and MB4 dense-graded mixes (6.0, 6.0, and 6.3 percent respectively) were lower than the optimum binder contents used in the mix designs of the gap-graded mixes (7.4, 7.1, and 7.2 percent respectively), with all mix designs performed following standard Caltrans methods.
- The results of limited shear testing of modified binders in dense-graded mixes (LMLC) indicate that the Permanent Shear Strain at 5,000 Cycles and Cycles to 5 Percent Permanent Shear Strain results for the dense-graded mixes indicated generally better rutting performance than those of the corresponding gap-graded mixes.

5.3. Reports

The following reports were prepared for this phase of the study:

- TSAI, B.W., Jones, D., Harvey, J., and Monismith, C. 2006. **Reflective Cracking Study: First-level Report on Laboratory Fatigue Testing.** Davis and Berkeley, CA: University of California Pavement Research Center. (UCPRC-RR-2006-08).
- GUADA, I., Signore, J., Tsai, B.W., Jones, D., Harvey, J., and Monismith, C. 2006. **Reflective Cracking Study: First-level Report on Laboratory Shear Testing.** Davis and Berkeley, CA: University of California Pavement Research Center. (UCPRC-RR-2006-11).

6. SECOND-LEVEL ANALYSIS

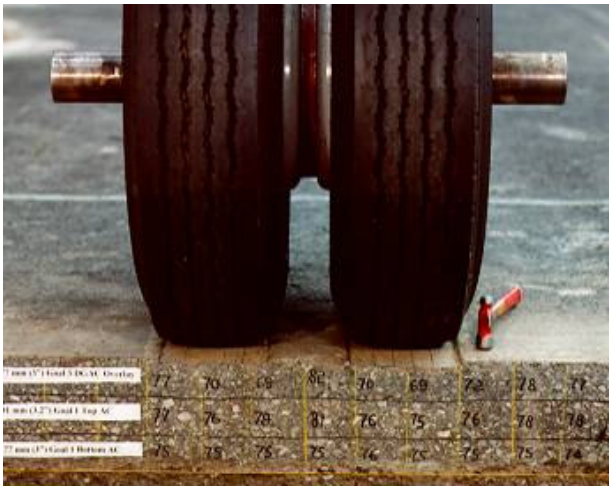

The second-level analysis consisted of a detailed study of the laboratory fatigue and shear results comparing the performance of the five mixes using a range of approaches, and a series of simulations using *CalME* mechanistic-empirical design software and continuum damage mechanics implemented using a finite element method. Simulations with these models were used for two purposes in this study:

- To simulate the HVS tests using uniform underlying support conditions, design thicknesses, and identical temperature conditions. These simulations were performed as a check on the results of the HVS test sections, which had some inevitable variability of testing conditions and deviations from the intended designs, to ensure that the conclusions did not change.
- To simulate the performance of other pavement structures functioning in different climate conditions. This permits extrapolation of the results of this project to a wider range of conditions, and will provide Caltrans with preliminary conclusions for implementation of the results in the field.

Findings were presented in one second-level analysis report (15).

6.1. Laboratory Fatigue and Shear

The main objective of the second-level analysis of the laboratory data was to compare the performance of the mixes with the five binders using the approaches and information gathered from assessments of:

- The stiffness deterioration process (or fatigue damage process) of a flexural controlled-deformation fatigue test of the mixes using a three-stage Weibull approach;
- The most appropriate parameters that identify fatigue performance, specifically the fatigue damage process used in comparing fatigue performance of different mixes;
- The permanent shear strain (PSS) accumulation processes of a controlled-load repetitive simple shear test at constant height (RSST-CH) of test results applied in the first level analysis using a three-stage Weibull approach, and

- The most appropriate parameters that identify rutting performance used in comparing rutting performance of different mixes.

6.1.1 Findings and Discussion

Use of Three-Stage Weibull Analysis to Characterize Fatigue and Shear Tests

The fitting of flexural controlled-deformation fatigue test results with a three-stage Weibull equation appeared promising. The three-stage Weibull equation is flexible and sufficiently precise to accommodate most fatigue damage curve shapes, while adequately characterizing fatigue performance in terms of the entire damage process. Conventional two-point fatigue life modeling considers only initial (50^{th} load repetitions) and end (50 percent stiffness reduction) points and neglects the fatigue damage process. For mixes using modified binders, the traditional parameter of 50 Percent Loss of Initial Stiffness does not capture the improved crack propagation resistance of rubber- and polymer-modified mixes that occurs after this point (Figure 6.1). In addition, test duration to reach 50 percent stiffness reduction is very long and thus not feasible. Hence, to accurately characterize the fatigue performance of these mixes, understanding the fatigue damage process is important.

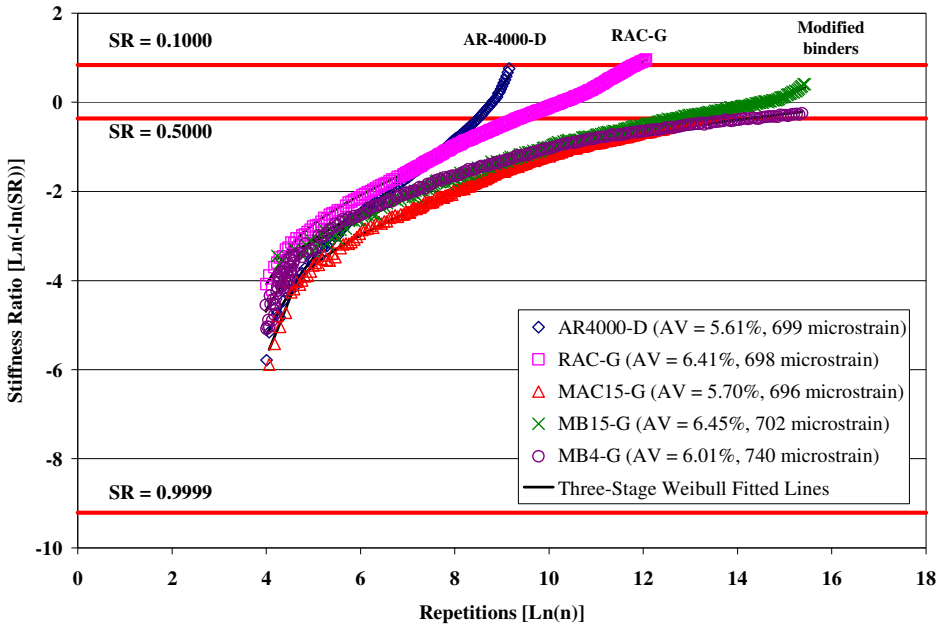

Figure 6.1: Typical Weibull curves for Reflective Cracking Study mixes.
20°C and 700 microstrain.

The fit of a controlled-load repetitive simple shear test with the three-stage Weibull equation was also satisfactory and provided an even better fit than that of a flexural controlled-deformation fatigue test, especially at Stage III.

Most Appropriate Parameters Identifying Fatigue and Shear Performance

The intercept and slope parameters of Stages II and III of a three-stage fatigue/shear Weibull curve ($\ln\alpha_2/\beta_2$ and $\ln\alpha_3/\beta_3$) can be used for characterizing both fatigue and shear performance in a consistent way, with increasingly negative values corresponding to improved performance for both flexural fatigue tests and repeated shear tests. This can be summarized as follows (Table 6.1):

Table 6.1: Summary of Parameters Identifying Fatigue and Shear Performance

Test	Parameter	Indicator of	Interpretation
Fatigue	$\ln\alpha_2/\beta_2$	Crack initiation performance	Increasingly negative values = improved performance
	$\ln\alpha_3/\beta_3$	Crack propagation performance	Increasingly negative values = improved performance
Shear	$\ln\alpha_2/\beta_2$	Early trafficking performance	Increasingly negative values = improved performance
	$\ln\alpha_3/\beta_3$	Later trafficking performance	Increasingly negative values = improved performance

Comparison of Fatigue and Shear Performance

Vector performance plots are considered useful for comparing the fatigue and shear performance of each mix when they are subjected to the effects of aging, air-void content, and gradation. As expected, the plots show that mixes that perform well in controlled-deformation beam fatigue do not perform well in shear and vice versa. Care needs to be taken when interpreting results from small data sets.

Figures 6.2 and 6.3 show the performance contour plots of fatigue and shear test results as well as the overall mean of each mix. The plots show that the contour line values appear to be a linear combination of the $\ln\alpha_3/\beta_3$ and $\ln\alpha_2/\beta_2$ parameters. Accordingly, the ranking of fatigue and shear performance, from best to worst differs from the findings presented in the previous chapter as follows:

Beam Fatigue		Shear	
1	MB4-G	1	MAC15-G
2	MAC15-G	2	AR4000-D
3	MB15-G	3	RAC-G
4	RAC-G	4	MB4-G
5	AR4000-D	5	MB15-G

In the ranking of shear performance, the mean positions of the MAC15-G, AR4000-D, and RAC-G mixes are very close with no apparent differences. The MB4-G and MB15-G mixes are also in the same contour band with the MB4-G mixes, appearing to perform slightly better than the MB15-G mixes.

One possible disadvantage of using $\ln\alpha_3/\beta_3$ and $\ln\alpha_2/\beta_2$ as the parameters to identify fatigue and shear performance is that independent testing variables such as temperature, stress/strain, and air-void content are embedded in the parameters, which can limit assessment of the influence of individual variables on material performance. The two parameters thus become functions of the independent testing variables, thereby potentially losing the connection between independent test variables and material performance.

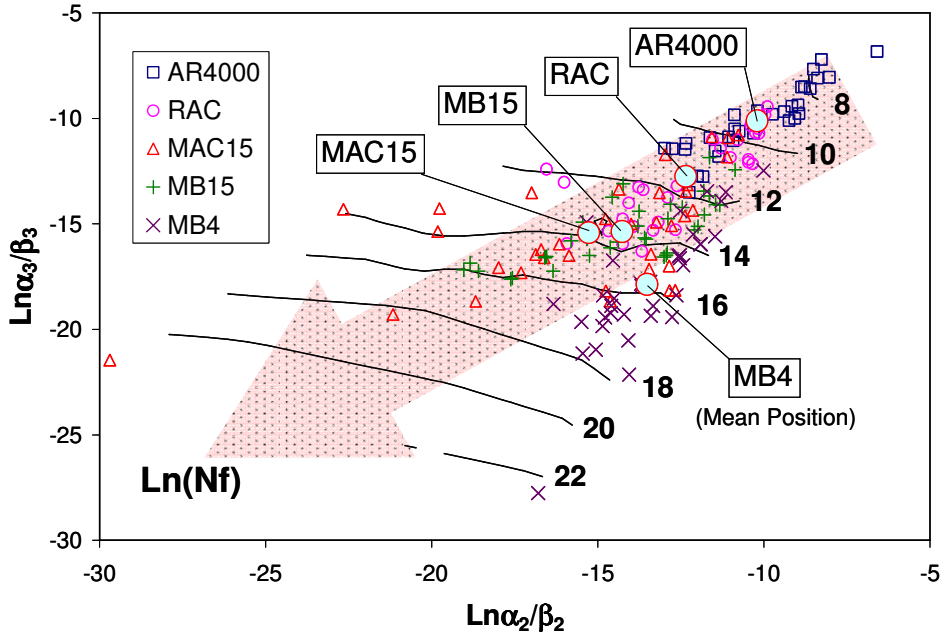

Figure 6.2: Identification of fatigue performance from lnα_3/β_3 and lnα_2/β_2 parameters.

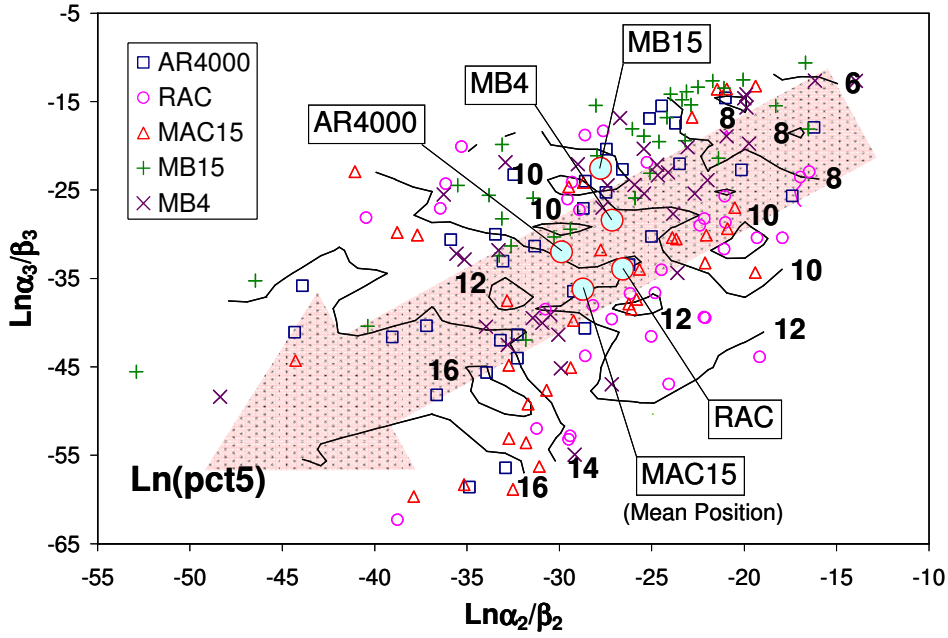

Figure 6.3: Identification of shear performance from lnα_3/β_3 and lnα_2/β_2 parameters.

Figure 6.4 shows the pruned dendrograms of lnα_3/β_3 and lnα_2/β_2 for fatigue and shear test results in this experiment. The following can be interpreted from the figure:

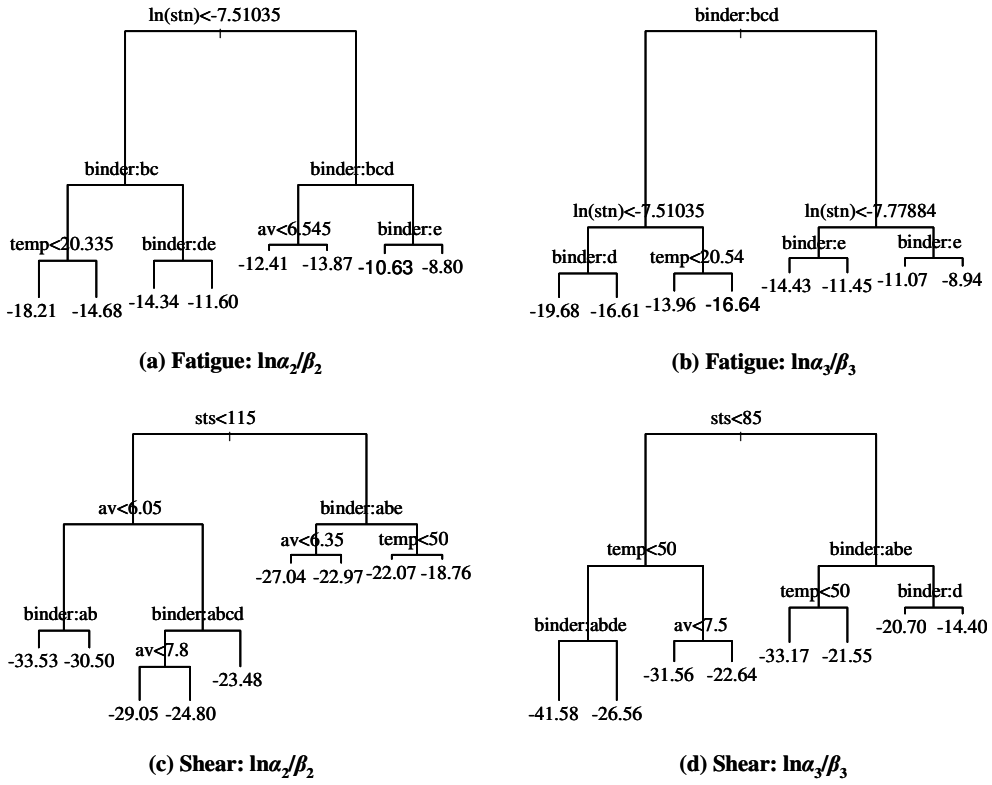

Figure 6.4: Pruned dendrograms of fatigue and shear three-stage Weibull parameters.

Fatigue

- The value of $\ln\alpha_2/\beta_2$ at Stage II of a fatigue Weibull curve is primarily affected by strain level, secondly by binder type, and then by air-void content and temperature.
- At Stage III, the values of $\ln\alpha_3/\beta_3$ are first determined by binder type and then by strain level.

Shear

- Stress level was the most significant factor affecting values of both $\ln\alpha_2/\beta_2$ and $\ln\alpha_3/\beta_3$.
  - At stress levels of 70 kPa (10 psi) and 100 kPa (14.5 psi), the air-void content critically affects the values of $\ln\alpha_2/\beta_2$, with lower air-void contents resulting in increasingly improved shear performance as indicated by more negative values of $\ln\alpha_2/\beta_2$.
  - At a stress level of 130 kPa (19 psi), binder type has the biggest influence on the values of $\ln\alpha_2/\beta_2$.
  - In Stage III, at a stress level of 70 kPa (10 psi), the values of $\ln\alpha_3/\beta_3$ are mainly affected by temperature, with lower temperatures resulting in increasingly better performance as indicated by more negative values of $\ln\alpha_3/\beta_3$.
  - At stress levels of 100 kPa (14.5 psi) and 130 kPa (19 psi), binder type has the biggest influence on $\ln\alpha_3/\beta_3$.

Table 6.2 summarizes the first-, second-, and third-level covariates (first level being most important) that affect the values of the $\ln\alpha_2/\beta_2$ and $\ln\alpha_3/\beta_3$ parameters for the fatigue and shear test results. The table shows that strain level contributes most to crack initiation (Stage II), and that binder type contributes most to the shape of the crack propagation curve (Stage III). Stress level has the biggest influence on shear damage in both stages, with the effects of air-void content and temperature also contributing.

Table 6.2: Summary of the Covariates for Parameters that Identify Performance
(Note: Importance is first level > second level > third level).

Category	Parameters	First Level	Second Level	Third Level
Fatigue	$\ln\alpha_2/\beta_2$	Strain level	Binder	Temperature, air-void content, binder
	$\ln\alpha_3/\beta_3$	Binder	Strain level	Binder, temperature
Shear	$\ln\alpha_2/\beta_2$	Stress level	Air-void content, binder	Binder, air-void content, temperature
	$\ln\alpha_3/\beta_3$	Stress level	Temperature, binder	Binder, air-void content, temperature

6.2. Mechanistic-Empirical Performance Simulations

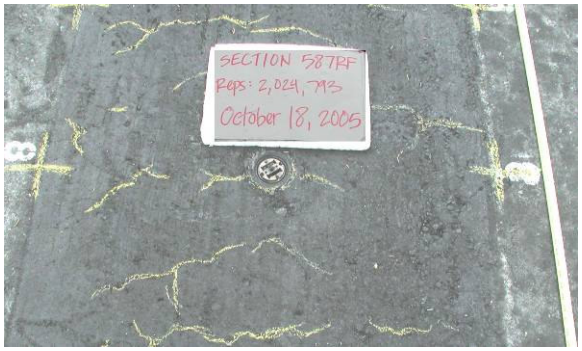

This study entailed the simulation of the HVS tests on the test track and a hypothetical set of typical Caltrans structures and traffic conditions in different climate regions in the state, using the California mechanistic-empirical design and analysis software *CalME*. The simulations were divided into six parts:

1. Simulation of the tests on the original pavement structure using actual (in-situ) conditions;
2. Simulation of the high-temperature rutting tests on the overlaid pavement structure using actual conditions;
3. Simulation of the moderate-temperature cracking tests on the overlaid pavement structure using actual conditions;
4. Simulation of the high-temperature rutting tests on the overlaid pavement structure using design thicknesses for the overlays and identical conditions of underlying pavement structure and temperature across all of the tests;
5. Simulation of the moderate-temperature cracking tests on the overlaid pavement structure using design thicknesses for the overlays and identical conditions of underlying pavement structure and temperature across all of the tests; and
6. Simulation of rutting and cracking for a hypothetical set of typical Caltrans structures and traffic conditions in different climate regions in the state.

The first three sets of simulations served to validate the *CalME* models by comparing the calculated results from *CalME* models with the measured responses and performance. Simulations 4 and 5 provided objective ranking of the different asphalt overlays without the influence of underlying conditions, which varied in the actual HVS tests. The sixth set of simulations provided extrapolation of the HVS results to field conditions and an understanding of the sensitivity of the predicted performance of the different overlays.

6.2.1 Fatigue of Asphalt Concrete Layers: Actual Conditions

The damage calculated by *CalME* compared to the observed cracking on the test sections was reasonably accurate, but the results were influenced by differences in the modulus of the underlying DGAC determined from Falling Weight Deflectometer (FWD) backcalculation and those determined from laboratory frequency sweep testing. This difference was attributed to early damage of the DGAC layer.

In order to obtain a better fit to the measured reflective cracking, the parameters in the equations developed for crack initiation and crack propagation in *CalME* were modified in a series of iterations, using different constants, to the values shown in Equations 6.1 through 6.4. Cracking predicted using these equations is compared to the measured cracking in Figures 6.5 and 6.7 and as a function of the observed reflective cracking in Figures 6.6 and 6.8.

$$\omega_{initiation} = \frac{1}{1+\left(\frac{h_{AC}}{350mm}\right)^{-1.9}} \quad \textbf{(6.1)}$$

$$Cr\,m/m^2 = \frac{10}{1+\left(\frac{\omega}{\omega_o}\right)^{-6}} \quad \textbf{(6.2)}$$

$$\omega_{initiation} = \frac{0.42}{1+\left(\frac{h_{AC}}{250mm}\right)^{0}} \quad \textbf{(6.3)}$$

$$Cr\,m/m^2 = \frac{10}{1+\left(\frac{\omega}{\omega_o}\right)^{-3.8}} \quad \textbf{(6.4)}$$

where: $\omega_{initiation}$ is the damage at crack appearance at the surface,
h_{AC} is the thickness of the asphalt concrete,
$Cr\,m/m^2$ is surface cracking density in m/m^2 of pavement,
ω is the calculated damage, and
ω_o is a constant.

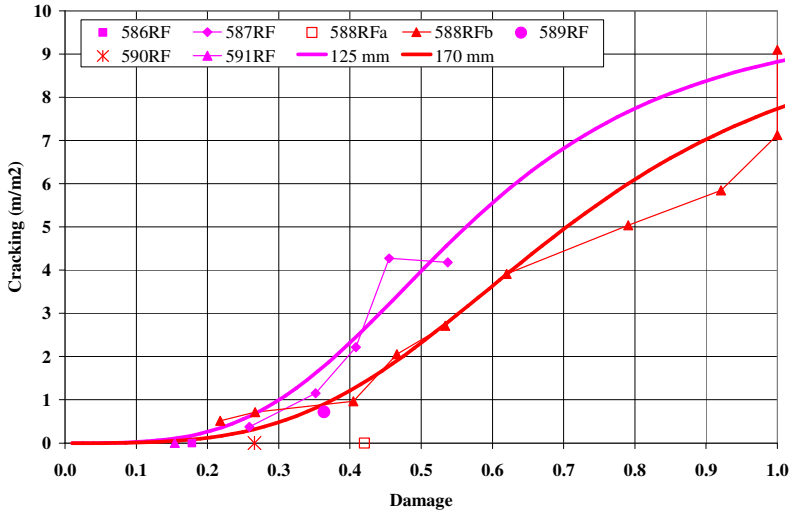

Figure 6.5: Observed reflective cracking vs fatigue damage using modified parameters (Eqs. 6.1/6.2).

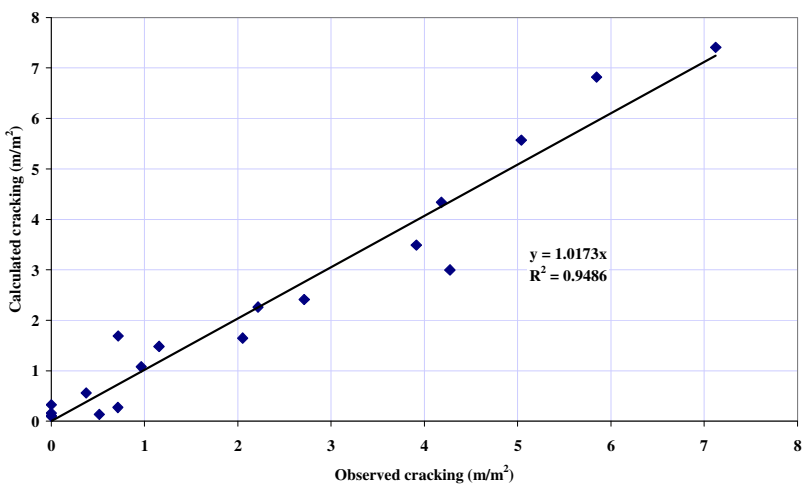

Figure 6.6: Predicted vs observed reflective cracking, using modified parameters (Eqs. 6.1/6.2).

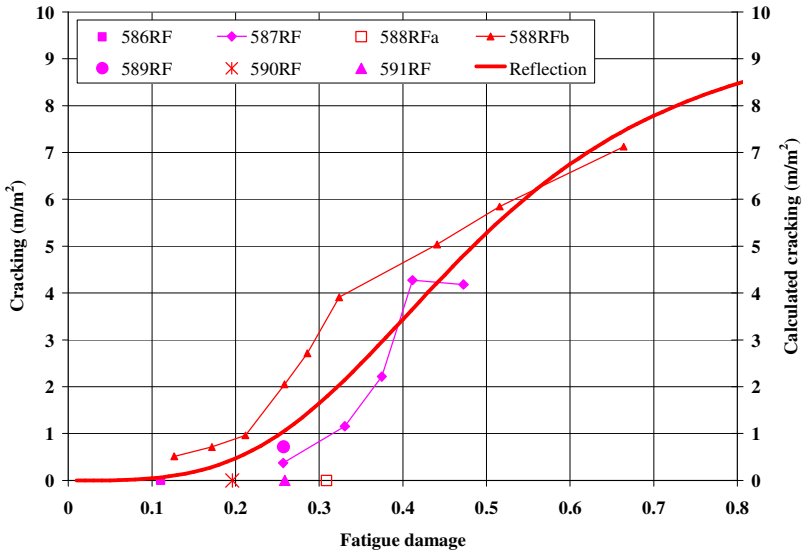

Figure 6.7: Observed reflective cracking vs fatigue damage using modified parameters (Eqs. 6.3/6.4).

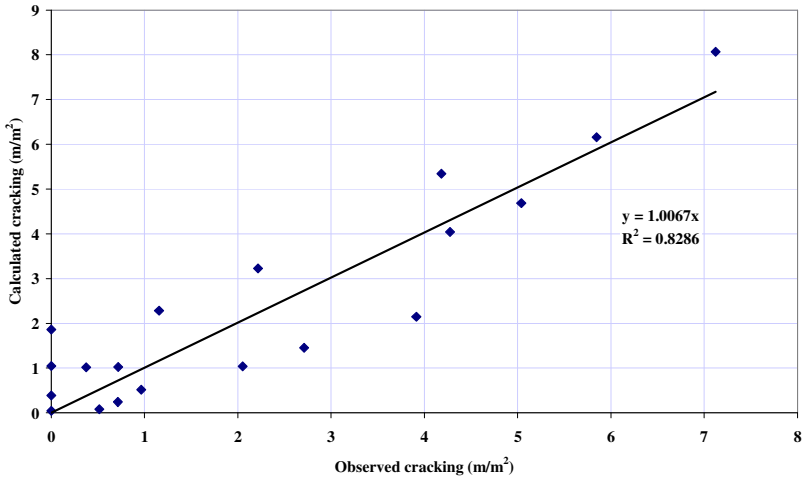

Figure 6.8: Predicted vs observed reflective cracking, using modified parameters (Eqs. 6.3/6.4).

6.2.2 Permanent Deformation: Actual Conditions

The terminal overall permanent deformation calculated by *CalME* at the end of each HVS test and the average measured down rut (same as average deformation in Table 4.5) from profile measurements are shown in Figure 6.9.

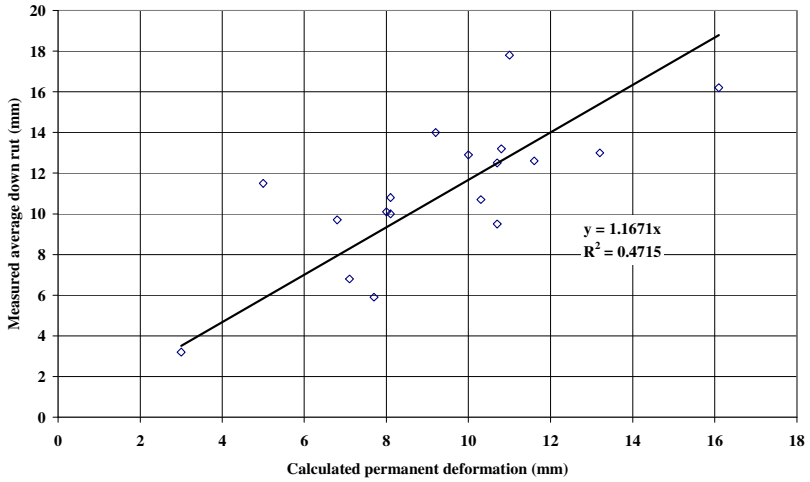

Figure 6.9: Calculated overall permanent deformation versus measured final down rut.

On average, *CalME* underestimated the overall permanent deformation by about seven percent, but the correlation coefficient was quite low. This should be seen in the light of the very large variation of down rut within some of the HVS sections. A difference of 5 mm (0.2 in.) to 10 mm (0.4 in.) between the minimum and the maximum down rut measured within the 6.0-m (19.7-ft) long test section was not unusual, and in one case (45 mm MB4-G) it reached 30 mm (1.2 in.).

Figure 6.10 shows the final permanent deformation at the top Multi-Depth Deflectometer (MDD) module as calculated by *CalME* and as measured. Whereas the resilient deflections at the surface (Road Surface Deflectometer [RSD]) and at the top MDD module are very similar, this was not the case for the permanent deformation which, in many cases, was mostly in the asphalt concrete layers and therefore not recorded by the MDDs, the sensors of which were positioned in the base rather than the surface due to space limitations in the relatively thin asphalt layers.

The permanent deformation of the top MDD comprises the permanent compression of the aggregate base layers and the permanent deformation of the subgrade. The permanent deformation of the subgrade is usually very low, less than 1.0 mm (0.04 in.). In two cases, 587RF and 589RF, one of the MDDs recorded final permanent deformations at the subgrade of 2.5 mm (0.1 in.) and 1.5 mm (0.06 in.), respectively. In both cases, however, another MDD recorded a permanent deformation close to zero. The calculated values were 0.8 mm (0.03 in.) and 1.3 mm (0.05 in.), respectively.

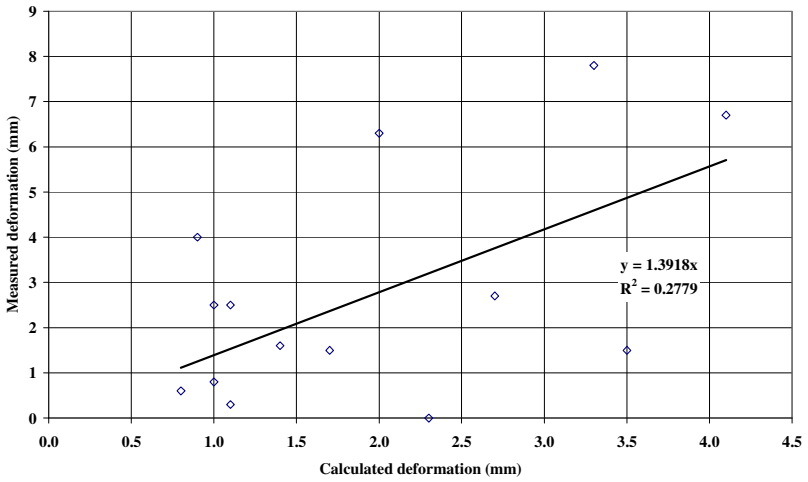

Figure 6.10: Calculated final permanent deformation of top MDD versus measured value.

An approximate value for the permanent compression of the asphalt concrete layer(s) can be obtained by subtracting the permanent deformation of the top MDD module from the average down rut, although it should be recalled that the first value is from one to three test points and the latter is the average over the whole 6.0-m (19.7-ft) long test section (except where the section was split into two subsections). In addition the MDDs were not exactly at the asphalt concrete/base interface. The calculated permanent deformation of the individual asphalt concrete layers and the measured thickness of the layers are shown in Figure 6.11.

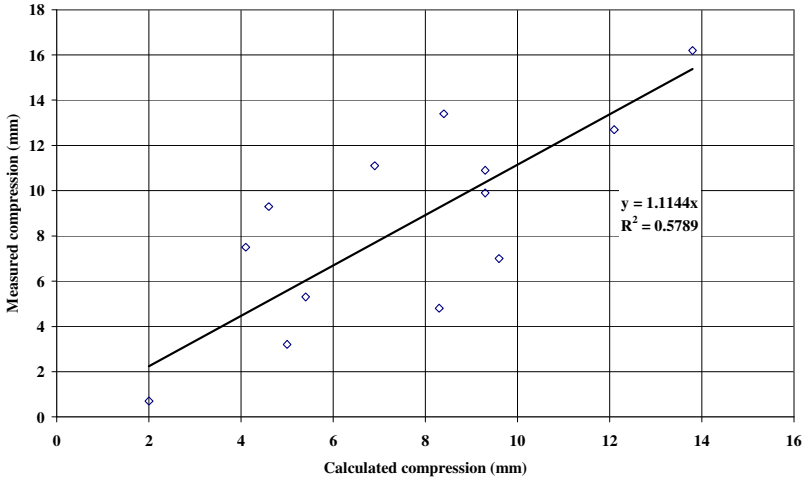

Figure 6.11: Calculated final compression of AC from profile and MDD versus measured value.

6.2.3 Simulation of Overlaid Sections (Uniform Conditions): Rutting Study

Experience has shown that the HVS testing conditions always have some influence on the performance of a particular section. This influence increases with increasing duration of the test. The rutting study was considered to consist of short duration tests since the test sections were on parts of the overlays that had not been trafficked previously with the HVS. As a consequence, the influence of the test conditions was

less pronounced than it was in the fatigue experiment, which had a longer duration and took place on test sections located precisely above those trafficked with the HVS during Phase 1 of the experiment. For completeness, the simulations were repeated for the rutting experiment using the same underlying structure used for the reflective cracking study discussed above, with the exception that the modulus of the underlying asphalt was assumed to be 3,200 MPa (464,120 psi) at 20°C (68°F), corresponding to the approximate layer moduli determined from FWD tests. The pavement structure and test conditions for HVS Test 584RF (90-mm MB4-G) were used for the simulation of uniform conditions. Almost 20,000 load repetitions (60 kN [13,500 lb]) were applied to this section. The ranking from best to worst was:

1. 90 mm MB4-G
2. AR4000-D
3. RAC-G
4. MAC15-G
5. 45 mm MB4-G
6. MB15-G

6.2.4 Simulation of Overlaid Sections (Uniform Conditions): Cracking Study

Although the original pavement was built to provide uniform support for the reflective cracking study, the forensic investigation showed that there was some variation over the length of the structure, specifically with regard to layer thickness, composition of the recycled aggregate, and degree of recementation of the aggregate particles. The conditions of the underlying structure, wheel loads, and climate should be identical when ranking the different overlays. The simulations were therefore repeated using uniform conditions. The HVS loading and climate for Section 591RF (MAC15-G) were used, but the number of load applications was multiplied by 50. Thicknesses of 45 mm, 80 mm, and 400 mm were used for the overlay, underlying DGAC, and base respectively. Moduli of 3,581 MPa, 400 MPa, and 100 MPa were used for the underlying DGAC, base, and subgrade respectively. An intact modulus of 12,000 MPa (1.7 million psi) with a damage of 0.253 was assumed for the underlying DGAC. The aggregate base and the subgrade were assumed to have stiffness factors equal to 0.8 and 0.46, respectively, and to have nonlinearities of +0.6 and -0.3, respectively.

Damage and cracking were determined at the end of the (simulated) HVS loading, at 458 million ESALs. Cracking was calculated using Equations 6.1 and 6.2. The values, ranked according to the amount of cracking from best to worst, are shown in Table 6.3. Fatigue damage was calculated based on the maximum tensile strain at the bottom of the overlay or at the bottom of the original asphalt layer. The maximum value at the beginning of the simulation is at the bottom of the original asphalt, but after a certain amount of damage further fatigue damage can be controlled by the strain at the bottom of the overlay, depending on the thickness and moduli of the layers. The strain at the bottom of a 45-mm (1.8-in.) thick overlay would typically be very small, and normally less than the strain at the bottom of the original asphalt layer. Therefore, the controlling strain would be at a depth of 125 mm (4.9 in.). The

opposite may be true for a 90-mm (3.5-in.) overlay, where the controlling strain would be at a depth of 90 mm. Under these circumstances, the resulting damage will be larger for a 90-mm overlay than for a 45-mm overlay, which explains the higher damage simulated on the 90-mm MB4-G overlay compared to the 45-mm MB4-G overlay.

Table 6.3: Ranking of Overlays after Increasing Damage

Rank	Layer	Damage	Cracking (m/m^2 [ft/ft^2])
1	MAC15-G	0.48	3.1 [0.9]
2	MB4-G (45 mm)	0.56	5.0 [1.5]
3	MB4-G (90 mm)	0.75	5.5 [1.7]
4	MB15-G	0.69	6.7 [2.0]
5	RAC-G	0.76	7.4 [2.3]
6	AR4000-D	1.00	7.7 [2.4]

The simulated reflective cracking is shown as a function of the number of loads (in ESALs) in Figure 6.12. The ranking depends to some extent on the number of load applications. The ranking would not change significantly if it was based on the reflective cracking predicted from fatigue damage of the overlay.

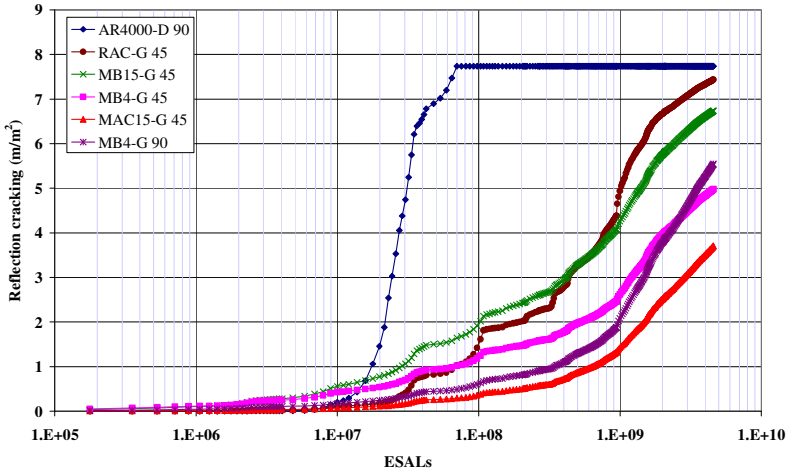

Figure 6.12: Simulated damage for identical testing conditions.

6.2.5 Extrapolation to Field Conditions and Sensitivity Analyses

These simulations were carried out to assess extrapolation of mix performance in the HVS tests to performance in the field. These results only provide a preliminary assessment of expected field performance. They include the many limitations of the modeling and need to be checked with results from in-service pavements. Based on the simulation results, the following observations were made:

- For reflective cracking performance of field-mixed, laboratory-compacted mixes in asphalt concrete overlays under field climate conditions:
  - The relative ranking with respect to reflective cracking under field conditions was the same as the ranking under HVS test conditions, with the exceptions being the RAC-G and MB15-G

mixes. RAC-G performed better than MB15-G in the field simulations, but worse in HVS tests.

- None of the mixes were sensitive to climate conditions.
- Increasing the overlay thickness from 45 mm (1.7 in.) to 90 mm (3.5 in.) significantly increased reflective cracking life.
- Reflective cracking life decreased as traffic volume increased.
- Increasing the traffic speed from 10 km/h (6 mph) to 70 km/h (44 mph) only slightly increased the reflective cracking life.

- For rutting performance of field-mixed, laboratory-compacted mixes in asphalt concrete overlays under field climate conditions:
  - The relative ranking with respect to rutting under field conditions (1→MAC15, 2→MB4, 3→AR4000, 4→RAC, 5→MB15) was different from the ranking under HVS test conditions (1→AR4000, 2→MB4, 3→RAC, 4→MB15, 5→MAC15).
  - The RAC-G and MB15-G mixes had better reflective cracking performance but worse rutting performance when compared to the AR4000-D mix.
  - Only the RAC-G and MB15-G mixes were sensitive to climate conditions.
  - Increasing the overlay thickness from 45 mm (1.7 in.) to 90 mm (3.5 in.)significantly increased the rutting life.
  - Rutting life decreased as traffic volume increased.
  - Increasing the traffic speed from 10 km/h (6 mph) to 70 km/h (44 mph) increased rutting life. This effect was especially significant for RAC-G and MB15-G mixes.
- For reflective cracking performance of asphalt concrete overlays using laboratory-mixed, laboratory- compacted mixes at 20°C (68°F):
  - The performance ranking was consistent with that observed for field-mixed, laboratory compacted mixes in different climate zones.
  - Gap-graded mixes with rubber modified binders generally performed better than dense-graded mixes with the same binders, except MB15, the performance of which did not depend on aggregate gradation.
- For rutting performance of asphalt concrete overlays using laboratory-mixed, laboratory-compacted mixes at 20°C (68°F):
  - The performance ranking was consistent with that observed for field-mixed, laboratory-compacted mixes in different climate zones.
  - Mixes with good reflective cracking performance tended to have good rutting performance.
  - Performance did not appear to be significantly dependent on aggregate gradation.

6.3. Continuum Damage Mechanics Simulations

This study entailed the simulation of the HVS tests on the test track using non-local continuum damage mechanics (CDM) implemented using a finite element method (FEM). This is a more sophisticated method than layer-elastic theory and provides greater insight into the crack propagation process and local-versus-global damage (i.e., damage under the wheel versus damage away from the wheel). However, it requires faster computation than can currently be accommodated in a design and analysis method to be used in practice. The simulations are divided into three parts:

- Calibration of the simulation procedure using actual in situ conditions of different overlays as model inputs and matching model predictions with observed reflective cracking performance for the HVS cracking tests on the overlaid structure at moderate temperatures;
- Simulation of the reflective cracking performance of the different asphalt concrete overlays observed from the HVS tests using uniform design thicknesses, underlying pavement structures, and temperatures; and
- Simulation of reflective cracking performance for a hypothetical set of typical Caltrans structures and traffic conditions in different climate regions in the state.

6.3.1 Calibration of the Simulation Procedure

The simulation procedure was found to predict the relative reflective cracking lives of asphalt concrete overlays in the project with reasonable accuracy. It was also found that the difference in the underlying pavement layers led to significantly different reflective cracking performances within each test section. It is therefore important to account for the effect of underlying layers when comparing the reflective cracking performance of different overlays.

6.3.2 Simulations Using Uniform Conditions

The effects of overlay thickness on reflective cracking life are shown in Figure 6.13. Increasing the overlay thickness from 45 mm (1.7 in.) to 90 mm (3.5 in.) increased the reflective cracking life by between 30 and 70 percent for all the mixes except the AR4000-D, the reflective cracking life of which was essentially the same for both overlay thicknesses. This indicates that the benefits of increasing the overlay thickness from 45 mm to 90 mm are insignificant and cannot be distinguished by the model used.

The effects of aggregate base stiffness are shown in Figure 6.14. Increasing the base stiffness (from 150 MPa to 300 MPa [21,750 psi to 43,500 psi]) increased reflective cracking lives significantly for all the asphalt concrete mixes. Improvement ranged from an 80 percent increase in life for the AR4000-D mix to a 230 percent for the MAC15-G mix. The overall ranking of reflective cracking performance is listed in Table 6.4.

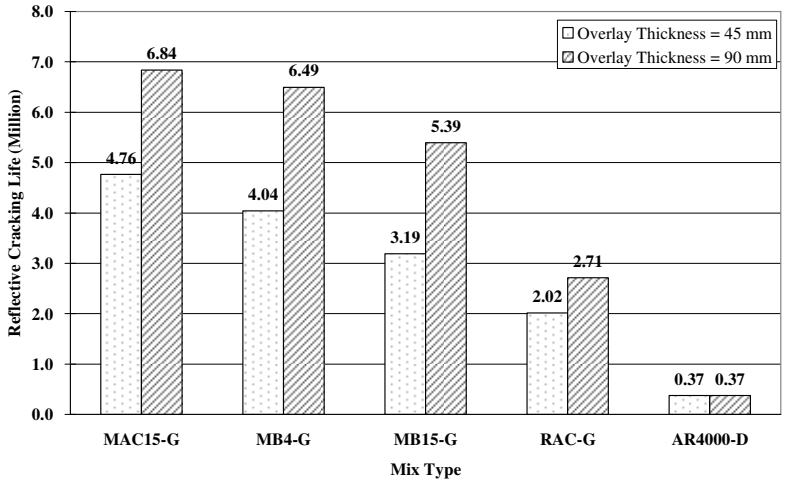

Figure 6.13: Effects of overlay thickness on relative reflective cracking life for different mixes.

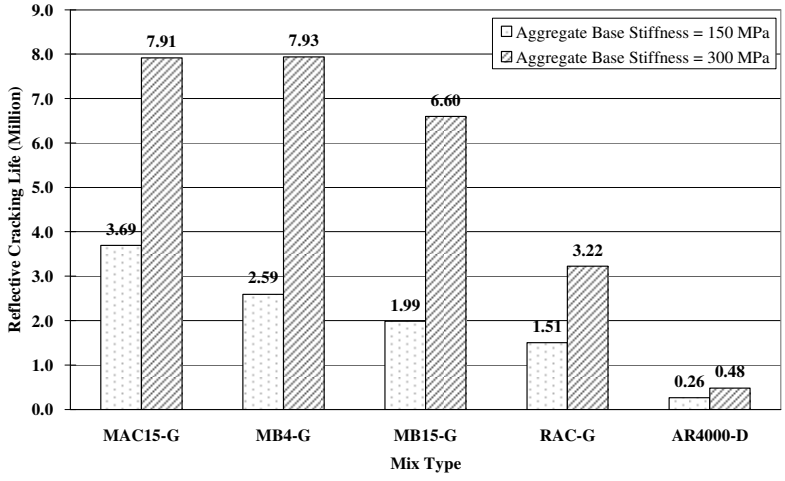

Figure 6.14: Effects of base stiffness on relative reflective cracking life for different mixes.

Table 6.4: Ranking of Reflective Cracking Performance of Asphalt Concrete Mixes
(based on simulations and uniform conditions)

Performance Ranking (Best to Worst)	Overlay Mix Type	Normalized Reflective Cracking Life
1	MAC15-G	1.00
2	MB4-G	0.91
3	MB15-G	0.74
4	RAC-G	0.41
5	AR4000-D	0.06

6.3.3 Extrapolation to Field Conditions and Sensitivity Analyses

These simulations extrapolate mix performance in HVS tests to performance in the field. However, the results only provide a preliminary assessment of expected field performance, include the many limitations of the modeling, and should be checked with field results. Based on the results of the simulations, the following observations were made:

- For field-mixed, laboratory-compacted mixes in asphalt concrete overlays under field climate conditions:
  - The relative ranking with respect to reflective cracking under field conditions was the same as the ranking under HVS test conditions, with the exception being the RAC-G and MB15-G mixes. RAC-G performed better than MB15-G in the field simulations but worse in the HVS tests.
  - AR4000-D and MB15-G mixes had significantly shorter reflective cracking life under the Desert climate than under South Coast and Central Valley climates. The other mixes did not appear to be sensitive to climate conditions.
  - Reflective cracking life was generally not sensitive to an increase in overlay thickness from 45 mm (1.7 in.) to 90 mm (3.5 in), and thus increasing the overlay thickness from 45 mm to 90 mm would not necessarily result in a longer reflective cracking life.
  - Reflective cracking life decreased as traffic volume increased.
  - Increasing traffic speed from 10 km/h (6 mph) to 70 km/h (44 mph) approximately doubled the reflective cracking life for the AR4000-D and MB15-G mixes. However, the reflective cracking life for MB4-G, MAC15-G, and RAC-G mixes were less sensitive to traffic speed.
- For asphalt concrete overlays using laboratory-mixed, laboratory-compacted mixes at 20°C (68 F):
  - Overlays with mixes using MB4, MB15, and MAC15 binders generally did not fail in reflective cracking after fifteen years of traffic, with the only exceptions being the MB15-G mixes, and MAC15-D mix.
  - A critical thickness (between 90 mm [3.5 in.] and 120 mm [4.7 in.]) exists below which increasing the overlay thickness did not influence reflective cracking life.
  - The effect of aggregate gradation on reflective cracking life depended on mix stiffness. Dense gradation was better for softer mixes (i.e., MB15), while gap gradation was better for stiffer mixes. For mixes that have adequate stiffness (i.e., MB4), aggregate gradation had no significant effect on reflective cracking performance.

6.4. Reports

The following report was prepared for this phase of the study:

- JONES, D., Tsai, B., Ullidtz, P., Wu, R., Harvey, J. and C. Monismith. 2007. **Reflective Cracking Study: Second-Level Analysis Report.** Davis and Berkeley, CA: University of California Pavement Research Center. (UCPRC-RR-2007-09).

7. CONCLUSIONS AND RECOMMENDATIONS

This report provides a summary of the thirteen reports prepared during the course of the Reflective Cracking Study, which together document an investigation undertaken to validate Caltrans overlay strategies for the rehabilitation of cracked asphalt concrete.

This work was conducted by the University of California Pavement Research Center as part of Partnered Pavement Research Center Strategic Plan Element 4.10: "Development of Improved Rehabilitation Designs for Reflective Cracking." Originally requested by the Caltrans/Industry Rubber Asphalt Concrete Task Group (RACTG), this work aims to compare the performance of one set of examples of thin overlays of cracked asphalt pavement that contain different types of binders modified with recycled tire rubber. The study is part of a more comprehensive work plan prepared by the Task Group that includes evaluation of pilot projects and construction and monitoring of field test sections; undertaken by other contractors.

Five binders were assessed during the study, including MB4, MB4 with minimum 15 percent recycled tire rubber, MAC15TR with minimum 15 percent recycled tire rubber (all terminal blended), asphalt rubber binder (ARB), and AR4000 (approximately equivalent to PG64-16). The asphalt rubber (field blended) and AR4000 binders were included for control purposes.

7.1. Conclusions

The following conclusions are drawn from the results of this study, organized by the study objectives agreed to by the RACTG, and documented in the project work plan prepared at the beginning of the study. All of these conclusions are based on the set of one example of each binder at one binder content, included in the experiment design.

Objective 1: Develop Improved Mechanistic Models of Reflective Cracking

Two sets of mechanistic-empirical models were developed for reflective cracking as part of this study:

- One set of models is based on the use of layer-elastic theory, and has been incorporated into the mechanistic-empirical pavement design and analysis software, *CalME* (final calculations were

made using Version December-2007. Version 0.95 (beta version) will be delivered to Caltrans in June 2008 when documentation is completed). *CalME* is being developed under the technical supervision of a Caltrans technical working group under the direction of the Division of Design, and is intended to be used as a design and analysis tool by Caltrans engineers and their consultants.

- The second set of models, which does not have a formal name and is not intended as a full-scale design tool by Caltrans, is based on the finite element method and continuum damage mechanics. It is a more sophisticated method that provides greater insight into the crack propagation process and local-versus-global damage (i.e., damage under the wheel versus damage away from the wheel) than does the use of layer-elastic theory. However, it requires faster computation than can currently be accommodated in a design and analysis method to be used in practice. The findings from comparison of the results of modeling individual crack propagation with these models are being used to enhance the models used in *CalME.*

Objective 2: Calibrate and Validate Mechanistic Models

Results from a comprehensive HVS study, during which more than 15 million load repetitions equating to about 400 million Equivalent Standard Axle Loads, and a comprehensive laboratory study, during which about 480 Repeated Simple Shear and Flexural Fatigue Beam tests were completed, were used together with results from other studies to calibrate and verify the models discussed above. Conclusions for this objective include:

- Both mechanistic-empirical models described in Objective 1 were calibrated and validated using the laboratory and HVS data generated in this study, as well as several data sets from other HVS tests and test tracks. The calibrations resulted in models that predicted the performance of the sections in terms of calculated-versus-measured deflections, changes in stiffnesses, and ranking of reflective cracking performance. The overall approaches were validated when it was shown that use of the same calibrated coefficients across all the different tests sections resulted in good matches between predicted performance and measured performance.
- It was found during calibration that bonding was a significant variable in predicting the actual performance of several HVS test sections where forensic evidence showed that layers had become unbonded. The reason for the debonding is uncertain because the same tack coat was applied to all sections at the same time. This conclusion emphasizes the need for continued use and improvement of effective bonding strategies. It also emphasizes the need for mechanistic-empirical analysis methods to explicitly consider the extent of bonding.
- The methods of characterizing the fatigue damage process in the mechanistic-empirical design models developed in this project were successful in predicting the performance of mixes with

modified and rubberized binders. The fatigue damage curve characterization of laboratory data and the incremental-recursive damage updating approach successfully modeled the significantly better crack propagation resistance of these mixes. In particular, the modified binder mixes tended to have laboratory fatigue damage curves that showed a decreasing rate of damage during propagation, whereas the conventional AR4000 dense-graded mix had an increasing damage rate during the propagation phase. This is a significant improvement over traditional mechanistic-empirical analysis approaches, which tended to underpredict the reflective cracking performance of these mixes.

- A forensic investigation of the HVS rutting tests showed that most of the shear deformation actually occurred in the underlying asphalt concrete layer and not in the overlays, although the ranking of the total HVS rutting followed the laboratory shear deformation resistance test results of the overlay mixes. The mechanistic-empirical models for rutting of the asphalt layers predicted the overall rutting performance ranking of each section, but did not fully capture the distribution of rutting between the overlay and the underlying asphalt layers. It is not clear whether the relative lack of aging and trafficking of the underlying asphalt layers (light car traffic and fewer than five delivery trucks per day at the HVS test site over three years) before placing the overlay influenced this behavior. It is also not clear whether this phenomenon occurs on in-service pavements, where longer loading periods, lighter traffic loads, and more years of age-hardening in the underlying asphalt layers differentiate them from HVS tests. These HVS results and model predictions suggest the need for forensic investigation of several rutted field pavements with thin rubberized and modified binder mixes and/or HVS rutting tests of thin overlays placed on aged field pavements.

Objective 3: Evaluate the Most Effective Strategies for Reflective Cracking

A more detailed analysis of the laboratory results and a series of simulations with the calibrated mechanistic-empirical models were used to evaluate which strategies had the best reflective cracking performance. Conclusions for this objective include:

- Second-level analysis of the fatigue and shear laboratory test data using three-stage Weibull analysis identified significant differences in the crack initiation and propagation performance, and the shear deformation resistance of the different mixes under various conditions. The performance with respect to fatigue and shear were combined using similar parameters into a single plot. This approach can be used in the future by designers for considering the relative risks of fatigue and shear, and in considering the effects of aging and gradation. This is an improvement on past strategies, which do not always optimize both shear and fatigue performance aspects for a given application.

- Although the laboratory shear test results correlated well with the observed rutting performance under the HVS, the results showed the importance of using mechanistic-empirical analysis to develop rutting- and cracking-performance estimates that consider the overlay material as well as its interaction with the rest of the pavement structure.
- Controlled-deformation fatigue beam testing used in this project was also found to match the reflective cracking of thin overlays for the structures tested by the HVS. However, the ranking of fatigue beam tests and predicted or actual field performance of thicker overlays and/or different pavement structures may differ because of interaction of the overlay with the pavement structure.
- The results of a limited exploratory laboratory experiment (included in the approved work plan) using modified binders in dense-graded mixes indicate that these mixes have lower cracking resistance, higher stiffness, and better rutting resistance compared with mixes with the same binders but using gap-gradation. This suggests that, apart from their use in thin reflective cracking overlays, the modified binders also hold promise for use in thicker structural overlays and new pavements. Mechanistic-empirical simulations for dense-graded modified binder mixes showed superior cracking resistance but poorer rutting resistance than conventional DGAC (now called hot-mix asphalt [HMA]).

Objective 4: Provide Recommendations for Reflective Cracking Overlay Strategies

Findings of the more detailed analyses of the laboratory shear and fatigue results, and the simulations with the calibrated models were used to prepare recommendations for reflective cracking studies. Conclusions for this objective include:

- Overall, the results indicate that when used as thin overlays on cracked pavement, the half-thickness modified binder mixes assessed in this study provide better performance with respect to reflective cracking than the full-thickness conventional dense-graded asphalt concrete (HMA). This is demonstrated by the absence of reflective cracking on the half-thickness modified binder overlays despite their being subjected to over a million more HVS repetitions than that required to crack the full-thickness AR4000-D overlay. The half-thickness RAC-G mix did not perform as well as the modified mixes but it still showed superior reflective cracking performance compared to the full-thickness AR4000-D, confirming results from previous HVS studies performed for Caltrans by the UCPRC.
- The re-analysis of the HVS fatigue test results using uniform underlying conditions, as opposed to the actual underlying conditions (which varied between HVS test sections) used during calibration, showed that the reflective cracking resistance of the modified and rubberized mixes in half-thickness overlays remained significantly better than that of the conventional dense-graded

asphalt concrete full-thickness overlay. This was found to be true using both mechanistic-empirical analysis approaches (*CalME* and continuum damage mechanics models).

- Re-analysis of the HVS rutting test results using uniform underlying conditions indicates that there is faster rutting of the asphalt layers when the modified mixes are used with slow traffic in hot climates. Performance should be assessed in pilot projects before wider use is considered under these conditions.
- Overall, the results indicate that the modified binder mixes (regardless of half or full thickness) assessed in this study have a greater risk of rutting under slow, heavy loads and hot conditions compared to the full-thickness conventional dense-graded asphalt concrete (HMA) overlay. The modified binder mix designs were performed using the same Hveem Stabilometer procedure used for RAC-G mixes. It is not known to what extent the rutting performance would have been improved, and conversely if the reflective cracking performance would have been affected, by using a different method that selected lower design binder contents.

7.2. Recommendations

Pilot Projects

The following recommendations with regard to the establishment of pilot projects are made based on the conclusions presented above:

- There is sufficient evidence from this study that a number of production-level pilot projects should be constructed using mixes with modified binders.
- Control mixes should be included in the pilot projects.
- Mixes used in the pilot projects should be subjected to laboratory testing and analysis of the type (reduced experiment design) used in this research project. This testing and analysis is needed to identify the range of performance for these mix types, which could not be measured with the one binder example in this study.
- The initial pilot projects with modified binder mixes should not be placed in locations with very hot climates and/or high traffic counts of slow, heavy trucks.
- The pilot projects should be established and monitored following the Pavement Preservation Study Technical Advisory Guide (PPSTAG [UCPRC-GL-2005-01]).

Testing and Analysis

The following recommendations with regard to testing and analysis are made based on the conclusions presented above:

- New mixes developed for reflective cracking, with either new gradations or new binders, should be evaluated with the laboratory testing and analysis techniques and the mechanistic-empirical

analysis models developed in this study. Based on the available research and performance data, additional HVS testing is not warranted before constructing and evaluating pilot projects, unless there is uncertainty from the modeling results for these new mixes.

- Laboratory investigation, additional analysis, and HVS validation is recommended to improve mix design procedures for rubberized and modified binder mixes. The mixes used in this study were designed using the Hveem Stabilometer with criteria (e.g., gradation) that were not consistent between mixes with conventional binders and mixes with rubberized and modified binders.
- Additional laboratory and modeling studies and HVS tests are also warranted to better assess the risk of rutting using mixes with these binders in thicker overlays, hot climates, and under slow, heavy loads, as well as the effects of changes to the mix design on reducing that risk. If field studies cannot be located for forensic evaluation of the ratio of rutting in the overlay and underlying asphalt layer, HVS testing of rutting of thin modified overlays on aged field pavements should be considered.

8. REFERENCES

1. **Generic experimental design for product/strategy evaluation** — crumb rubber modified materials. 2005. Sacramento, CA: Caltrans.
2. **Reflective Cracking Study: Workplan for Comparison of MB, RAC-G, and DGAC Mixes Under HVS and Laboratory Testing.** 2003. Davis and Berkeley, CA: University of California Pavement Research Center. (UCPRC-WP-2003-01)
3. BEJARANO, M., Jones, D., Morton, B., and Scheffy, C. 2005. **Reflective Cracking Study: Summary of Construction Activities, Phase 1 HVS Testing, and Overlay Construction**. Davis and Berkeley, CA: University of California Pavement Research Center. (UCPRC-RR-2005-03).
4. HARVEY, J., Du Plessis, L., Long, F., Deacon, J., Guada, I., Hung, D. and Scheffy, C. 1997. **CAL/APT Program: Test Results from Accelerated Pavement Test on Pavement Structure Containing Asphalt Treated Permeable Base (ATPB) – Section 500RF**. Davis and Berkeley, CA: University of California Pavement Research Center. (Report Numbers UCPRC-RR-1999-02 and RTA-65W4845-3).
5. JONES, D., Tsai, B.-W., and Harvey, J. 2006. **Reflective Cracking Study: First-level Report on HVS Testing on Section 590RF — 90 mm MB4-G Overlay.** Davis and Berkeley, CA: University of California Pavement Research Center. (UCPRC-RR-2006-04)
6. JONES, D., Wu, R., Lea, J., and Harvey, J. 2006. **Reflective Cracking Study: First-level Report on HVS Testing on Section 589RF — 45 mm MB4-G Overlay.** Davis and Berkeley, CA: University of California Pavement Research Center. (UCPRC-RR-2006-05)
7. WU, R., Jones, D., and Harvey, J. 2006. **Reflective Cracking Study: First-level Report on HVS Testing on Section 587RF — 45 mm RAC-G Overlay.** Davis and Berkeley, CA: University of California Pavement Research Center. (UCPRC-RR-2006-06)
8. JONES, D., Wu, R., and Harvey, J. 2006. **Reflective Cracking Study: First-level Report on HVS Testing on Section 588RF — 90 mm DGAC Overlay.** Davis and Berkeley, CA: University of California Pavement Research Center. (UCPRC-RR-2006-07)
9. JONES, D., Wu, R., and Harvey, J. 2006. **Reflective Cracking Study: First-level Report on HVS Testing on Section 586RF — 45 mm MB15-G Overlay.** Davis and Berkeley, CA: University of California Pavement Research Center. (UCPRC-RR-2006-12)
10. JONES, D., Wu, R., and Harvey, J. 2007. **Reflective Cracking Study: First-level Report on HVS Testing on Section 591RF — 45 mm MAC15-G Overlay.** Davis and Berkeley, CA: University of California Pavement Research Center. (UCPRC-RR-2007-04)

11. STEVEN, B., Jones, D., and Harvey, J. 2007. **Reflective Cracking Study: First-level Report on the HVS Rutting Experiment.** Davis and Berkeley, CA: University of California Pavement Research Center. (UCPRC-RR-2007-06)
12. JONES, D., Harvey, J., and Steven, B. 2007. **Reflective Cracking Study: HVS Test Section Forensic Report.** Davis and Berkeley, CA: University of California Pavement Research Center. (UCPRC-RR-2007-05)
13. LU, Q., Jones, D., and Harvey, J. 2007. **Reflective Cracking Study: Backcalculation of HVS Test Section Deflection Measurements.** Davis and Berkeley, CA: University of California Pavement Research Center. (UCPRC-RR-2007-04)
14. TSAI, B.-W., Jones, D., Harvey, J., and Monismith, C. 2006. **Reflective Cracking Study: First-level Report on Laboratory Fatigue Testing.** Davis and Berkeley, CA: University of California Pavement Research Center. (UCPRC-RR-2006-08)
15. GUADA, I., Signore, J., Tsai, B.-W., Jones, D., Harvey, J., and Monismith, C. 2006. **Reflective Cracking Study: First-level Report on Laboratory Shear Testing.** Davis and Berkeley, CA: University of California Pavement Research Center. (UCPRC-RR-2006-11)
16. JONES, D., Harvey, J. and Monismith, C. 2007. **Reflective Cracking Study: Second-Level Analysis Report.** Davis and Berkeley, CA: University of California Pavement Research Center. (UCPRC-RR-2007-09)